GL01227

Reprinted from
Economic Geology
Vol. 72, 1977, pp. 1471–1504

Irreversible Mass Transfer between Circulating Hydrothermal Fluids and the Mayflower Stock

R. N. Villas and D. Norton

Abstract

Heat and mass transport processes related to the Mayflower stock in the Park City district, Utah, have been simulated using calculations based on geological observations and numerical methods which approximate convective and conductive heat transfer in permeable media. Permeability and flow porosity values for the Mayflower stock were estimated on the basis of a planar fracture model and data on the abundances and apertures of continuous fractures. Estimated permeabilities ranged from 4×10^{-9} to 10^{-7} cm^2 and were hypothesized to represent initial permeabilities at the onset of the hydrothermal fluid circulation. An estimated fluid mass of 10^{13} kg/km strike length of the stock circulated through the upper 1.5 km of the Mayflower stock in 1.8×10^5 years of cooling, thereby reducing the thermal anomaly to 0.3 of its initial value. Temperatures decreased rapidly in the permeable portions of the stock, as a result of convective transfer of heat, but remained at 350° to 250°C in the upper 1.5 km for approximately 7×10^4 years subsequent to fracturing of the stock. Fluids in the host rocks flowed toward and often into the stock from distances about 5 km away from the stock side contact. Irreversible mass transfer between these circulating fluids and the Mayflower stock altered the stock to mineral assemblages which reflect the chemical composition of the rocks through which the fluids circulated, the pressure and temperature conditions along the flow paths, and initial composition of the fluids.

Simulation of the heat transport processes in the Mayflower system provides an initial approximation of the temperature, pressure, and fluid fluxes that may have been realized in the natural system. These data allow the mineral content of the altered Mayflower rocks to be predicted from mass transfer computations. Irreversible mass transfer reactions between the unaltered Mayflower rocks and solution compositions derived initially from fluid inclusion data were computed at discrete temperatures over the interval from 300° to 150°C. The alteration processes in the Mayflower stock were thus simulated by a sequence of isothermal reactions over the cooling history of the stock. The mineral content of the altered igneous rocks exposed in the Mayflower mine was determined by least-square treatment of bulk chemical compositions of rocks and mineral phases and was used to test the validity of coupling existing theoretical models of mass and heat transfer. The assumed solution compositions, prevalent temperature and pressure during the hydrothermal processes, and the estimated mass of fluids that circulated through the upper 1.5 km of the Mayflower stock as it cooled predicted masses of the mineral assemblages similar to those measured in the altered Mayflower igneous rocks.

The determined mineral modes disclose two broad zones over the north-south cross section of the mine: a lateral zone characterized by an increase of K-feldspar (3–15 wt %), kaolinite (0–10 wt %), and quartz (12–24 wt %), and a decrease of andesine (55–25 wt %) toward the main veins; and a vertical zone characterized by higher concentrations of K-feldspar, kaolinite, anhydrite, and pyrite below the 2,400-ft mine level, and calcite-quartz and biotite above. Gains and losses for elemental components indicate an overall loss (in grams of components per cm^3 of rock) of Si (0.009), Al (0.050), Na (0.032), and Ca (0.011) and an overall gain of Mg (0.026), K (0.020), S (0.038), SO_3 (0.037), and CO_2 (0.007). A relatively small gain of Fe (0.006) is the result of decrease in bulk density caused by the dissolution of igneous mafic minerals to produce pyrite, as evidenced by the shift from an annitic to a phlogopitic biotite during the hydrothermal event.

This analysis of the Mayflower hydrothermal system suggests that the original igneous minerals were altered by acid-sulfate, Na-K-rich solutions at moderate temperatures, < 400°C, and pressures, ≤ 1 kb. These solutions added large masses of Mg, K, S, and C to the stock and, concomitantly, altered the original igneous minerals. In order to account for the observed masses and compositions of alteration products, fluid fluxes on the order of 10^{-7} g/cm^{2}s are required for at least 2×10^5 years. This large mass ($\sim 10^{10}$ g/km^2 of area) of hydrothermal fluid was evidently derived from a variety of environments within and around the stock.

Introduction

TERTIARY plutons in the Cottonwood-Park City area, Utah, have intruded folded metamorphic and sedimentary units of Precambrian to Jurassic age. These intrusive rocks range in composition from quartz monzonite to quartz diorite and include the Little Cottonwood, Alta, and Clayton Peak stocks in the Cottonwood area and the Pine Creek, Mayflower, Ontario, Valeo, Flagstaff, and Glencoe stocks in the Park City district. This series of igneous events distributed over several millions of years were characterized by magma temperatures of approximately 850° ± 50°C. Each discrete intrusive body was apparently emplaced at approximately the same depth in the crust (<10 km below the surface), and its thermal energy was dispersed by conductive heat transfer and convective flow of aqueous solutions through the stock-host rock environment. The shallow depths of emplacement of these bodies into water-saturated permeable rocks suggest that convective fluid flow contributed significantly to the transport of heat and mass.

The emplacement of these relatively shallow-seated heat sources, and the subsequent fracturing that occurred in the Cottonwood-Park City area in Tertiary times, generated the physical conditions appropriate for fluid circulation that resulted in chemical reactions between original igneous materials and the circulating fluids, ultimately forming ore deposits and extensive hydrothermal alteration in the area.

Numerical simulation of heat transfer and chemical reaction between fluids and rocks at elevated temperature and pressure (Helgeson et al., 1970; Norton, 1972; Norton and Knight, 1977) suggests several parameters that must be documented in order to predict the nature of mineral deposition in pluton environments. The purpose of this communication is to present the results of preliminary studies whose objectives were to develop and test methods useful in quantifying these parameters. The first section of this paper analyzes the thermal and hydrodynamic aspects of the problem; the second section analyzes the hydrothermal alteration and mineral deposit formation.

Geology of the Cottonwood-Park City Area

The Cottonwood-Park City area is located in the central-northern part of the State of Utah, approximately 50 km southeast of Salt Lake City, at the intersection of the north-south-trending Wasatch Range and the east-west-trending Uinta Range. This region, in which rocks from Precambrian to

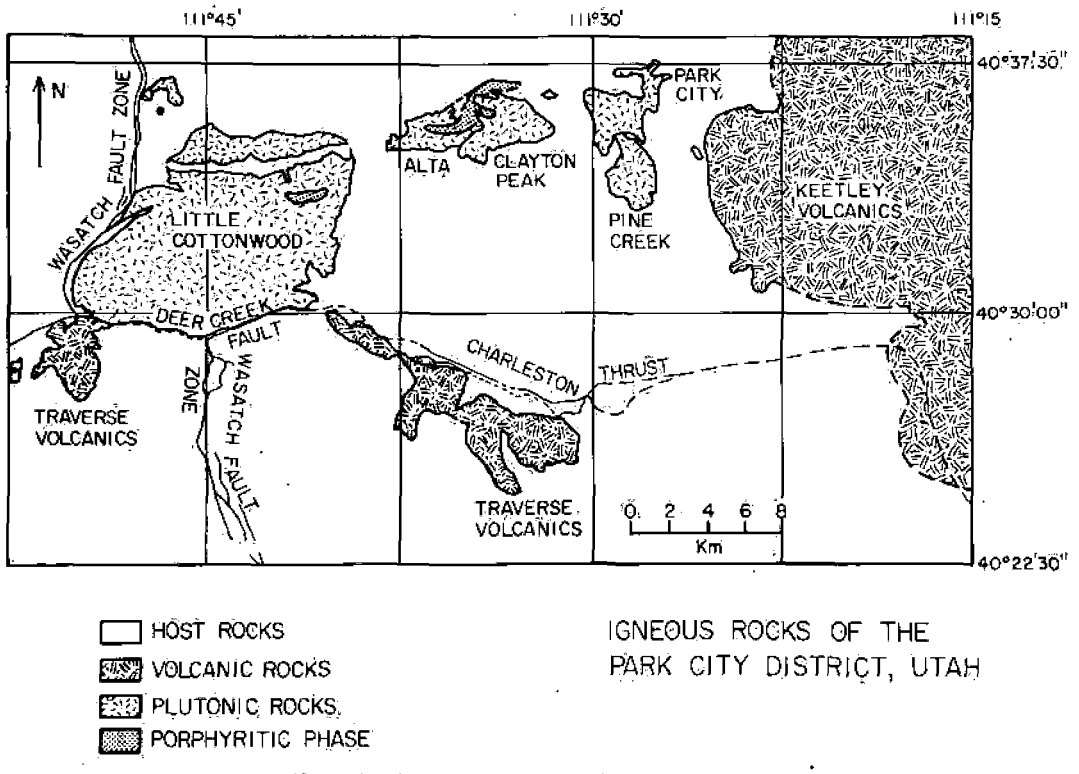

Fig. 1. Distribution of Tertiary igneous rocks in the Cottonwood-Park City area, Utah (modified after Crittenden et al., 1973).

Quaternary age crop out, has undergone two major uplifts: the Uinta on the east and the Cottonwood on the west. Gneiss, quartzite, and schist make up most of the Precambrian terrains and occupy the central parts of the above-mentioned uplifts. Paleozoic sedimentary rocks, which flank both uplifts, are largely composed of limestone, dolomite, and sandstone and their altered equivalents. Mesozoic rocks crop out away from the uplifts and include conglomerate, sandstone, shale, and limestone. Cenozoic rocks are irregularly distributed and include both intrusive and extrusive igneous rocks and sedimentary units. Tertiary plutonic intrusions occur along a line coincident with the east-west trend of the Uinta axis. The Eocene-Oligocene equivalents of these plutonic rocks occur on the east (Keetley volcanics) and on the west and south of the area (Traverse volcanics).

Intrusve rocks in the Cottonwood-Park City area occur as dikes and stocks discordantly emplaced into metamorphic and/or sedimentary host rocks (Fig. 1). They include, from west to east: the Little Cottonwood, Alta, Clayton Peak, and Pine Creek stocks and a composite intrusion comprising the Mayflower, Ontario, Valeo, Flagstaff, and Glencoe stocks (Bromfield et al., 1974), collectively called the Park City stock. These intrusions range in composition from quartz monzonite to quartz diorite, with these same variations frequently found within individual intrusions. Major mineral constituents are plagioclase (oligoclase-andesine), orthoclase, quartz, biotite, and hornblende, which vary in abundance from stock to stock. The Little Cottonwood, Clayton Peak, and Alta stocks are composed of coarse-grained rocks, in marked contrast with the Pine Creek and Park City stocks which are porphyritic and generally have an aphanitic or fine- to medium-grained groundmass. The Alta stock, however, displays a porphyritic phase which appears to intrude an enclosing nonporphyritic phase.

Chemical analyses of these intrusive rocks (Table 1) suggest a trend in silica content increasing to the west, although among the porphyritic intrusions the silica content is more or less constant. Radiometric dating of the igneous rocks indicates that magmatic activity in the area lasted a maximum of 17 m.y. in Oligocene-Miocene times and that the stocks become progressively younger to the west (Crittenden et al., 1973).

Several continuous fissures 4 km or more in length have been recognized in the Park City district (Fig. 2). They are normal faults that strike east-northeast–west-southwest and dip either northwest or southeast. The most prominent of these fissures is the Daly-Ontario-Hawkeye which extends

TABLE 1. Chemical Compositions of Igneous Rocks in the Cottonwood-Park City Area

	L. Cottonwood (1)	Alta (1)	Alta (1)	Alta (5)	Alta* (1)	Alta* (5)	Clayton Peak (4)	Clayton Peak (3)	Pine Creek (3)	Mayflower (2)	Ontario (3)	Flagstaff (3)
SiO_2	67.02	65.27	62.16	63.92	63.43	63.70	59.35	61.40	60.70	61.11	60.80	59.50
Al_2O_3	15.78	15.75	17.17	16.13	15.93	15.89	16.36	17.90	17.50	18.20	16.70	17.20
Fe_2O_3	1.56	2.31	2.26	2.03	2.61	2.09	2.90	2.90	3.05		3.96	2.66
FeO	2.80	1.85	2.78	2.43	2.31	1.97	3.36	2.06	1.89	3.93†	1.20	2.54
MgO	1.09	1.62	1.81	1.90	2.27	1.73	3.08	2.22	2.49	3.04	1.81	2.93
CaO	3.31	4.09	4.70	4.50	4.33	4.07	5.03	4.30	4.60	5.10	3.15	3.09
Na_2O	3.85	3.92	3.96	3.77	3.66	3.85	3.73	4.48	4.46	3.94	5.39	4.26
K_2O	3.67	3.25	3.58	3.24	3.49	3.19	3.85	2.40	2.54	2.95	3.60	2.37
H_2O^-	0.29	0.21	0.03	0.01	0.27	0.03	0.28	0.72	0.36		0.44	0.47
H_2O^+	0.63	0.53	0.60	0.44	0.74	0.49	0.64	1.64	0.64		0.73	2.32
TiO_2	0.37	0.55	0.53	0.61	0.62	0.53	0.87			0.82		
ZrO_2	0.04	0.02	0.01		0.03		0.03					
P_2O_5	0.26	0.25	0.17	0.31	0.16	0.25	0.44					
S	0.03		0.04					0.02	n.d.	0.12	0.07	n.d.
MnO	0.02	0.10	0.06	0.08	0.09	0.07	0.07			0.10		
CO_2		Trace			Trace					0.48		
BaO	0.13	0.11	0.17		0.15		0.16					
Cl		0.01			0.05		0.05					
FeS_2		0.02					0.02					
SrO		0.05					0.05					
SO_3										0.58		
Total	100.85	99.91	100.03	99.37	100.17	99.86	100.29	100.00	98.20	100.37	97.80	97.30

* Porphyritic phase.
† Total Fe as FeO.
n.d. = none detected.
References: (1) Calkins and Butler, 1943; (2) Villas, 1975; (3) Norton, unpub. data; (4) Boutwell, 1912; and (5) Wilson, 1961.

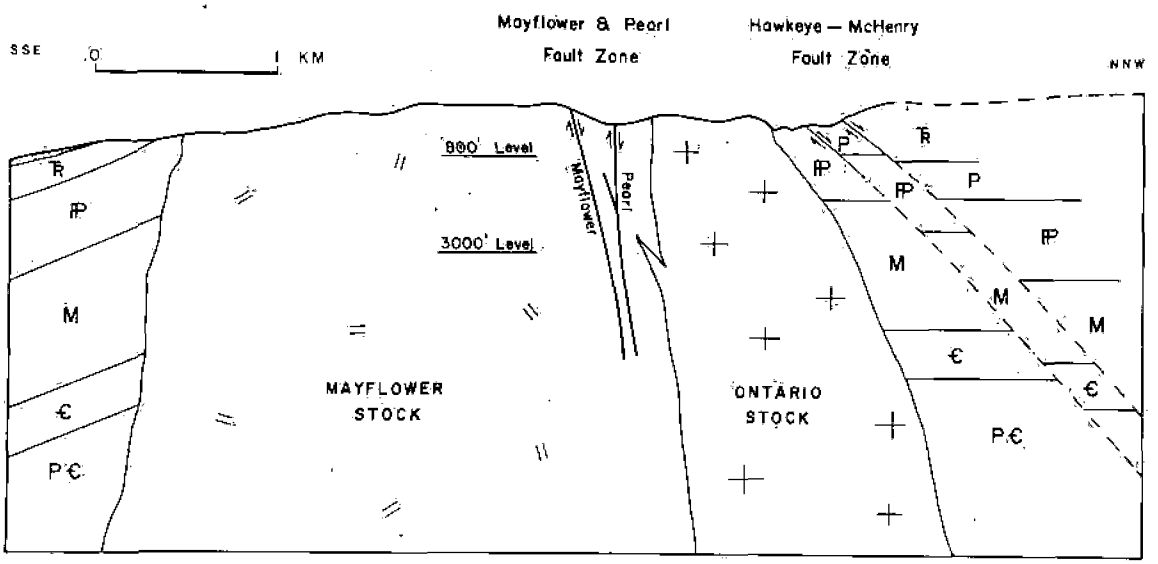

FIG. 2. Schematic north-northwest–south-southeast cross section of the Mayflower stock showing major geological features. Sedimentary units are represented with their maximum thickness. T = Triassic, P = Permian, P = Pennsylvanian, M = Mississippian, € = Cambrian, and, P€ = Precambrian.

for approximately 10 km from east of the Keetley volcanics to west of the Clayton Peak stock. Other regionally less continuous fissures, but locally important because of their associated ore deposits, are the Mayflower-Pearl, Naildriver, Back Vein, Crescent, and Massachusetts. Southeast-dipping faults, ranging from N 25° E to almost east-west, generally exhibit wider scatter in their strike directions than northwest-dipping faults; angles of dip vary from moderate (45°–55°) to steep (80°–90°) (Fig. 2).

An irregular pattern of fracturing in the host rocks between the Little Cottonwood stock and the Clayton Peak-Alta complex is indicated on the Dromedary Peak (Crittenden, 1965) and Brighton (Baker et al., 1966) geologic maps, but fractures apparently do not extend into the plutons. Their maps show that fractures, up to 1 km long and aligned parallel to the major fissures of the adjacent Park City district, transect the central portions of the Little Cottonwood stock. Likewise, most dikes cutting through the host rocks and plutons in the Cottonwood area follow the major fissure directions of that district. Similar structural relations, with fractures displaying two prominent sets, one along N 80° E directions and the other along N 25°–50° E directions, are present in the Alta stock. Fracture abundances in the Alta stock were estimated between one and three fractures per meter (Wilson, 1961). Similarly, reconnaissance observations of the fracture abundance in the Little Cottonwood and Clayton Peak stocks have revealed local zones where fracture abundances are approximately one fracture per meter.

The Mayflower Pluton

The hydrothermal systems in the Cottonwood-Park City area that developed as a consequence of emplacement of igneous intrusions can be simulated if hydrodynamic parameters are available. These properties were estimated for the Mayflower stock, which is well exposed in the extensive underground workings of the Mayflower mine, as described below.

The Mayflower pluton is the easternmost intrusion of the composite Park City stock, which has been emplaced into a sequence of intercalated clastic and carbonate units of Precambrian to Jurassic age. The post-Devonian formations include most of the carbonate beds and form a relatively thin cover overlying much thicker Precambrian and Cambrian strata. All of these sedimentary units have been broadly folded into the north-plunging Park City anticline, which has been truncated by intrusive rocks on its southern extension. Fissures developed in the area along east-northeast–west-southwest directions and localized the base metal ore deposits of the Park City mining camp.

The Mayflower pluton is exposed in the Mayflower mine between the 800-ft and 3,000-ft levels (Fig. 3). Underground workings show the Mayflower pluton in contact with sedimentary formations from the Mississipian Gardison limestone on the bottom of the Pennsylvanian Weber quartzite, on the surface (Quinlan and Simos, 1968), and with rocks

of two other stocks: the Ontario and the Valeo. Crosscutting relations between the Mayflower and the Ontario stocks show the former to be older, but age relationships to the Valeo stock are not evident.

Economic mineralization in the Mayflower stock occurs along the Mayflower-Pearl fault zone and consists of fissure-filling Pb-Zn sulfides with important amounts of gold, copper, and silver. Mine production has come primarily from veins in igneous host rocks; only about 20 percent of the production has been provided by veins and replacement deposits in sedimentary host rocks (Barnes and Simos, 1968).

Orientation, continuity, frequency, and aperture of fractures were determined for the Mayflower stock to serve a twofold objective: (1) analysis of the tectonic history of the stock with the hope of disclosing possible relationships with the major fissure zones of the Park City district; and (2) estimation of hydrodynamic properties on the basis of fracture continuity, frequency, and aperture.

Interpretation of the fracture pattern of the Mayflower stock with regard to the district structural framework was based on an analysis of 1,100 fracture planes, mostly shear, derived from Hecla Mining Company maps, together with fracture orientation data obtained during this study. The results of this analysis reveal that two prominent sets of fractures developed in the Mayflower stock (Figs. 4A and 4B). One set trends northeast-southwest, dipping either northwest or southeast; the other is northwest-southeast trending and dips dominantly southwest. The steep-dipping character of both fracture sets is evident from the stereogram plot of poles. For purposes of subsequent discussion, the representative structural attitudes of these two sets were considered to be N 50° E/80° NW and N 50° W/80° SW.

The northeast-trending fissure system in the Mayflower pluton is subparallel to the major fissure systems in the district (Figs. 2, 4A, and 4B). However, the northwest-trending fissures in the Mayflower pluton do not have recognized counterparts on a district scale. These fracture sets in the pluton are considered conjugate shear fractures developed during the pluton emplacement and cooling processes (Villas, 1975). The contemporaneity of the two sets is evidenced by the lack of significant offset of one fracture set by the other and the fact that both sets contain similar alteration mineralogy. The conjugate shear angle (2θ) of these two sets is approximately 80° ± 5°, measured from the stereograms (Figs. 4A and 4B). Failure under conditions of low coefficient of internal friction, [$\mu = \tan(90° - 2\theta)$], as indicated by the Navier-Coulomb's or Mohr's criterion of failure, is consistent with failure at high temperature and high confining pressure (Heard, 1967).

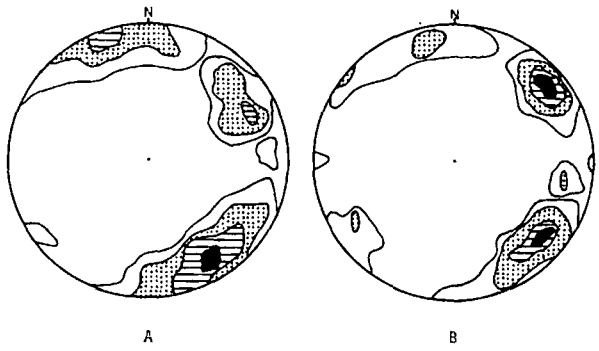

FIG. 4. Percent plot of the poles of fractures in the Mayflower and Ontario stocks. One percent counting areas. Lower hemisphere projection on equal area net. A. Approximately 1,100 sheer planes compiled from mine maps (all levels below the 700-ft level). Dark areas, 5.5 to 7.5 percent; hachured areas, 3.4 to 5.5 percent, dotted areas, 1.5 to 3.5 percent, and blank encircled areas, 0.5 to 1.5 percent. B. 21,061 poles of mineralized fractures (800-ft, 1,380-ft, 1,505-ft, 1,775-ft, 2,005-ft 2,200-ft, 2,600-ft, 2,800-ft, and 3,000-ft levels). Dark areas, 8.0 to 11.0 percent; hachured areas, 5.0 to 8.0 percent; dotted areas, 2.0 to 5.0 percent; and black encircled areas, 0.8 to 2.0 percent.

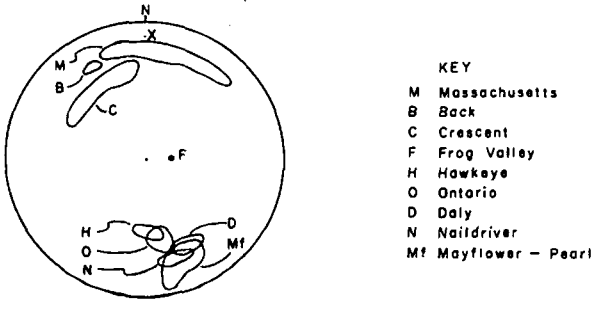

FIG. 3. Lower hemisphere stereographic plot of the poles of the major fissure zones present in the Park City district. Encricled areas delimit the variation of fissure attitude; X represents the axis of the Park City anticline.

Fluid flowpaths through fractured media are principally along continuous fractures which are usually present in the crystalline rocks, and an analysis of hydrothermal fluid flow through these rocks coupled with the reactions that occur between fluids and rocks requires consideration of those fracture properties which define rock permeability (Norton and Knapp, 1977). If the fractures are considered to consist of equidistant, planar, parallel plates of infinite extent, as proposed by Snow (1968, 1970), then the permeability (k, in cm^2, 10^{-8} cm^2 = 1 darcy) of a single set of fractures is given by:

$$k = \frac{n d_f^3}{12} \qquad (1)$$

where the abundance of continuous fractures (n, in cm^{-1}) and their apertures (d_f in cm) need to be known. The flow porosity (ϕ) per unit length of

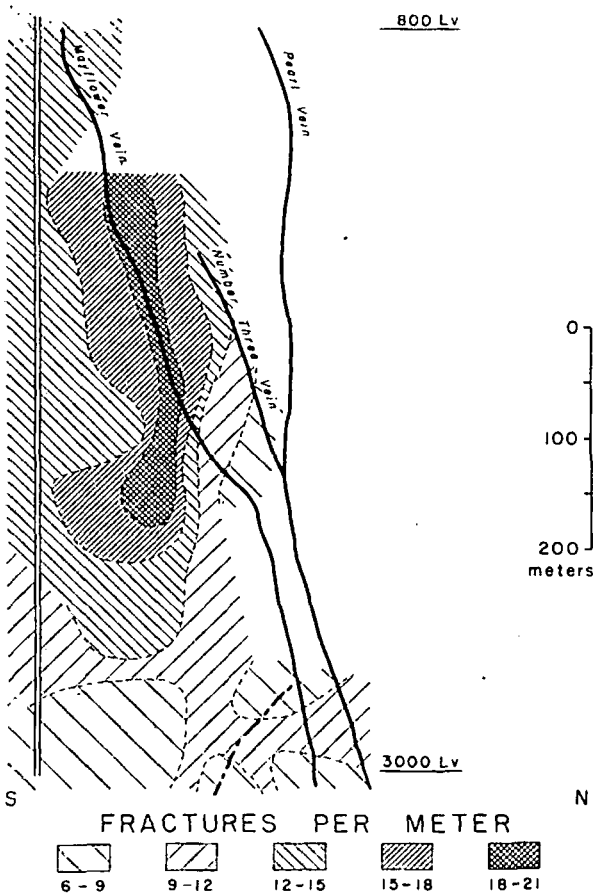

FIG. 5. Fracture abundance (n) distribution in a portion of the Mayflower stock showing the substantial decrease of n below the 2,600-ft level and zones of higher fracture density related to the Mayflower vein in the upper levels.

fracture for the corresponding case of equation (1) can be written as

$$\phi = nd_i. \qquad (2)$$

Fracture abundance and aperture were, therefore, measured and used with equation (1) to estimate the flow porosity and permeability of the Mayflower pluton. The abundance of continuous fractures (cf. Villas, 1975, for methods) over a north-south cross section of the Mayflower mine ranges from six fractures per meter to 21 fractures per meter (Fig. 5). These values are generally greater than those for all other stocks in the Cottonwood-Park City area, which are generally in the order of 0.6 to 3.0 fractures per meter. Larger fracture abundances in the Mayflower stock occur on the upper levels of the mine in the vicinity of the Mayflower vein, notably between the 1,380-ft and 2,005-ft levels where they occur symmetrically on either side of the vein. A substantial decrease in fracture abundance occurs below the 2,600-ft level.

The continuous fractures mapped in the Mayflower pluton were partially or totally filled with alteration minerals. Although present-day openings are most likely the net effect of mineral dissolution and precipitation, these openings are the only remaining indication of what the fracture apertures were during the alteration processes. Fracture aperture data for the Mayflower pluton refer to present-day openings and are assumed to represent the fracture aperture at the onset of the hydrothermal fluid circulation. In the absence of a more adequate way to quantify paleofracture apertures, this approach is considered to provide a reasonable initial estimate. Fracture aperture values measured in this manner range from 40 to 270 μm and average 145 μm (Villas, 1975). On some levels where the average aperture values are rather uniform, on the order of 150 μm $\pm$ 30 μm, no systematic variations in apertures with depth or lateral extent were found.

The geometry and distribution of pores define the contact area between fluids and reactant minerals—a critical parameter in understanding the mass transfer between reactant minerals and aqueous solutions. It is necessary, therefore, to discriminate the major

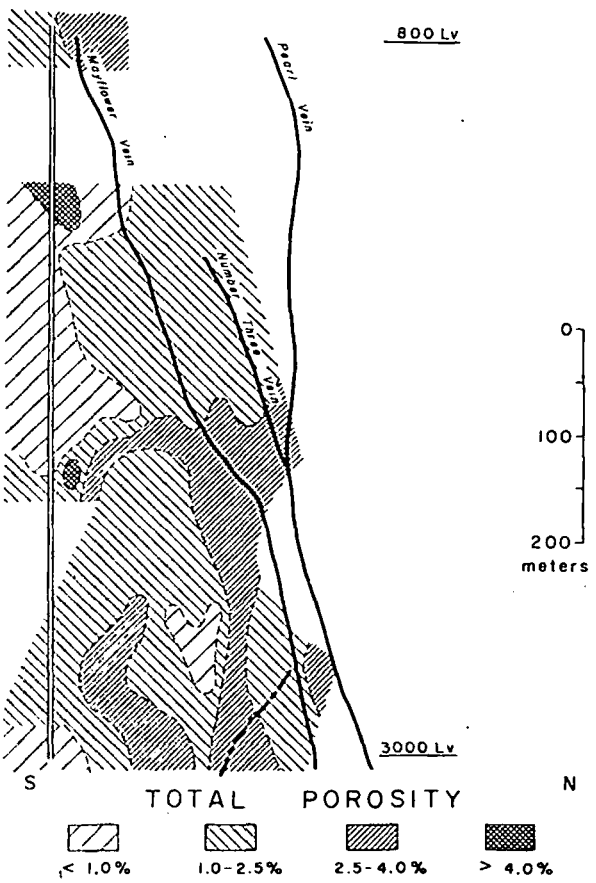

FIG. 6. Distribution of total porosity (ϕ_T) in the Mayflower stock.

contributing parts of the rock porosity. The nature of pores can be related to specific porosities,

$$\phi_T = \phi_F + \phi_D + \phi_R \quad (3)$$

where ϕ_T is the total porosity of the rock, and ϕ_F is the flow porosity which refers to open spaces along fractures where aqueous ions are transported primarily by fluid; ϕ_D is the diffusion porosity and includes those pores or dead-end fractures conected to flow chanels. This latter type of fluid-saturated void constitutes the channels through which ions are transported, primarily by diffusion. ϕ_R is the residual porosity which is associated with pores not connected to flow or diffusion channels, such as fluid inclusion voids, mineral grain boundaries, and submicroscopic cracks (Norton and Knapp, 1977).

Total porosity of a rock can be obtained from

$$\phi_T = 1 - \frac{\rho_B}{\rho_\gamma} \quad (4)$$

where ρ_B and ρ_γ are the bulk and grain densities of the rock, respectively. Values of total porosity for the Mayflower pluton fall in the range of 0.4 to 6.0 percent. Average total porosities for rocks along traverses oriented along east-northeast–west-southwest directions, at approximately 15 m south of the Mayflower vein, are the highest values (3.20%, 4.50%, and 2.70% for the 2,005-ft, 2,200-ft, and 2,600-ft levels, respectively), whereas those along north-south traverses on these same levels reveal average porosities of 2.20, 2.00, and 1.20 percent, respectively. The east-northeast–west-southwest traverses correspond to altered zones where clay minerals are most abundant. The distribution of total porosity values over a north-south cross section of the mine (Fig. 6) indicates that the higher values occur below the 2,005-ft level.

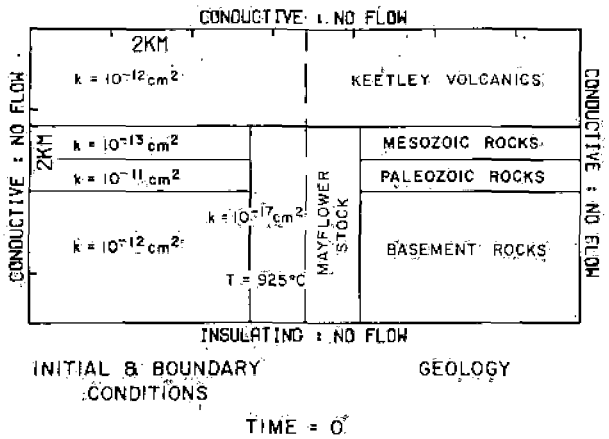

FIG. 7. Geology and initial boundary conditions used for the two-dimensional cooling model of the Mayflower stock.

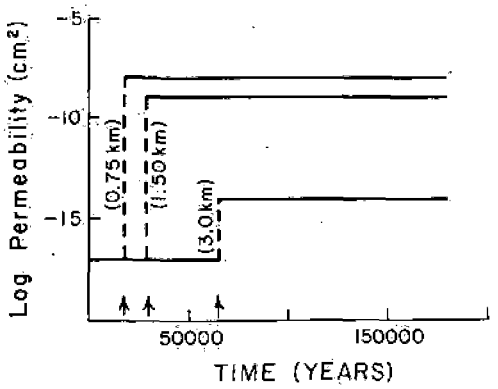

FIG. 8. Variation of permeability (k) with time throughout section down to 0.75, 1.50, and 3.0 km below the top of the Mayflower stock.

The directional permeabilities of the Mayflower pluton were computed with respect to the N 50°0 E/80° NW and the N 50° W/80 SW structural planes and were calculated from equation (1). Values range from $<10^{-14}$ to 7×10^{-8} cm² for fractures oriented along the N 50° E/80° NW direction and from $<10^{-14}$ to 5×10^{-8} cm² for the N 50° W/80 SW plane. These results are in reasonable agreement with reported values of permeabilities for fractured plutonic rocks. Permeabilities ranging from 10^{-19} to 1.7×10^{-7} cm² have been measured in quartz-porphyry stocks, although most reported values occur in the 10^{-19} to 10^{-9} cm² range (Cadek et al., 1968). This lower permeability range was attributed to the fact that those stocks are not as abundantly fractured and/or that the fractures observed are filled with alteration minerals.

Simulation of the Hydrothermal System Related to the Mayflower Stock

The hydrothermal system associated with the emplacement of the Mayflower and Little Cottonwood stocks has been simulated in order to predict the style of fluid circulation related to these intrusions. The large permeability of the Mayflower stock requires that convective fluid flow was the dominant mechanism of heat transport during its thermal history. By contrast, the Little Cottonwood stock is characterized by very large fracture spacings and, hence, low permeability, and appears to have cooled predominantly by conduction.

The system was simulated by methods which utilize numerical approximations of differential equations which describe the process of heat and mass transport around cooling plutons (Norton and Knight, 1977). The computational program affords for both conductive and convective heat transfer mechanisms in a two-dimensional framework, thermodynamic properties of the circulating fluid (H_2O system) in the

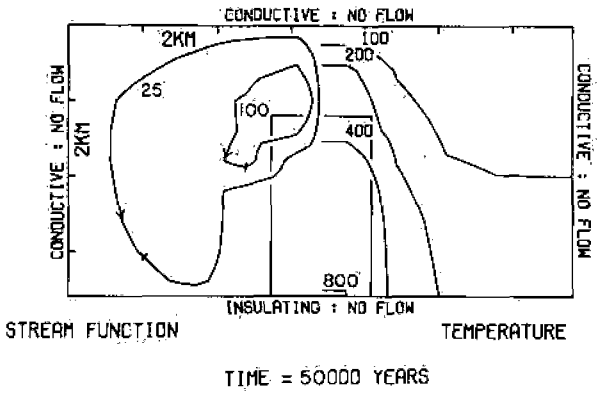

FIG. 9. Steady state (A) streamfunction and (B) isotherms in the Mayflower system at 5×10^4 years of cooling.

P-T region of interest, and variable permeabilities and thermal conductivities at each grid point of the domain.

Simplified geologic cross sections combined with estimates of permeabilities for the different rock units and temperature of the heat source define a possible set of initial conditions at the time of emplacement of the Mayflower stock (Fig. 7). Emplacement of the intrusion into water-saturated host rocks was assumed to be instantaneous. The initial temperature of the stock was set to 925°C, and the surrounding rocks were set to temperatures appropriate for a geothermal gradient of 20°C/km. Heat of crystallization, for water pressures compatible with the depths of emplacement, was included in the heat equations. The size and shape of the stocks were assigned on the basis of geologic cross sections and constraints imposed by the numerical approximations which utilize discrete points to approximate the differential equations. A thermal conductivity of 3.0×10^{-3} cal/cms °C was assumed for all rocks. The systems were analyzed for conductive boundary conditions, except for the lower boundary which was insulating, and impermeable flow boundary conditions were used.

Host rock permeabilities were assigned on the basis of notions of permeabilities of stratified sequences comparable to the varied lithologies in the Cottonwood-Park City area. Stock permeabilities, however, were estimated on the basis of observed fracture characteristics, as previously discussed. Initial permeabilities of the magma at the time of emplacement were assumed to be 10^{-17} cm^2. To account for variation of permeability with time, fracturing was simulated by instantaneously increasing the permeabilities as the stocks cooled below solidus temperatures, i.e., 750°C.

The style of fluid circulation caused by the emplacement of the Mayflower stock has been predicted on the basis of estimated permeabilities, as discussed earlier. Three episodes of fracturing were simulated as the stock cooled below 750°C, approximately the solidus temperature of this system. Each of these episodes was assumed to affect progressively lower zones of the stock (Fig. 8). Fractures developed during the first episode were considered to extend arbitrarily into the host rock for distances of 1.5 km away from the top and upper 0.75-km margins of the stock, and the host rock permeabilities were increased one order of magnitude relative to their initial values. Partial or total filling of fractures with alteration minerals is evident and indicates that rock permeabilities have actually decreased with time. Although this decrease may have had a substantial effect on the style of flow, it was not accounted for in this analysis.

Subsequent to fracturing, relatively large amounts of fluids circulated through the domain, with the exception of the impermeable lower half of the stock. As gradients in the streamfunction increased (Figs. 9 to 11), convection cells, initially centered

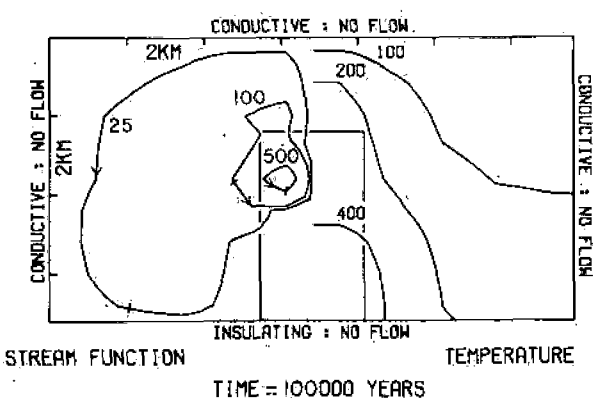

FIG. 10. Steady state (A) streamfunction and (B) isotherms in the Mayflower system at 10^5 years of cooling.

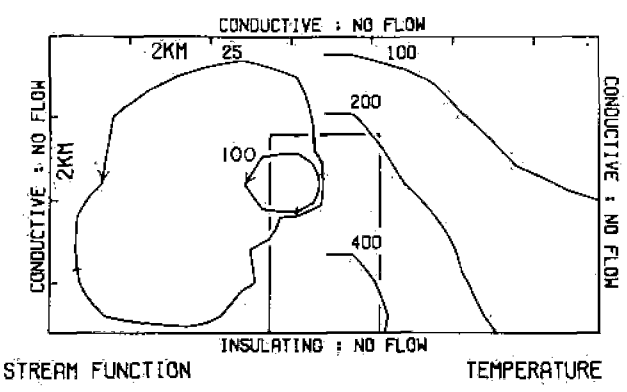

FIG. 11. Steady state (A) streamfunction and (B) isotherms in the Mayflower system at 1.8×10^5 years of cooling.

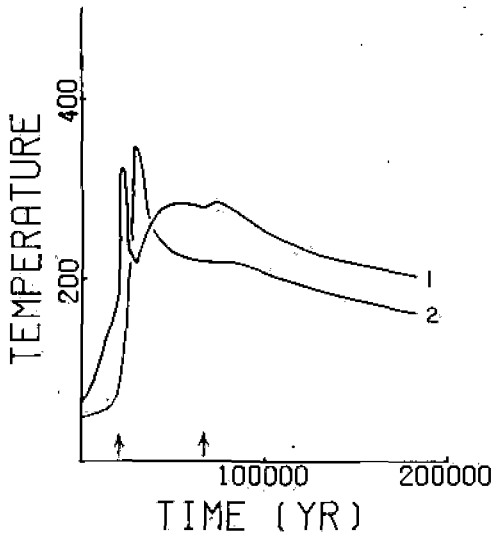

FIG. 12. Average temperature of a 2-km² region as a function of time in the Mayflower systems at fixed positions, 0.4 and 1.2 km, above top of the stock, 1 and 2, respectively. Arrows show times at which permeability was increased.

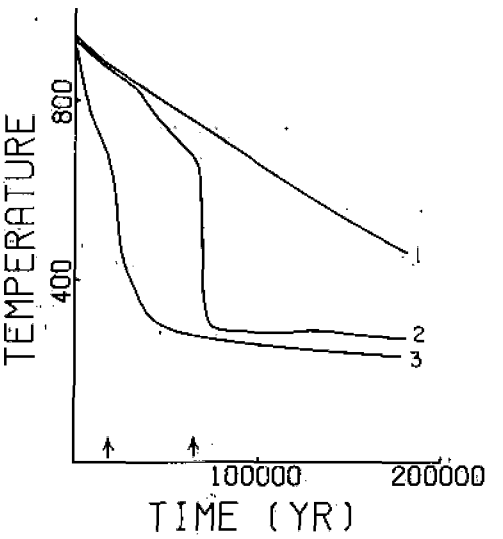

FIG. 13. Average temperature for 2 km² as a function of time in the Mayflower system at fixed positions, 3.6, 2.0, and 0.4 km, below top of the stock, 1, 2, and 3, respectively. Arrows show times at which permeability was increased.

in the host rocks, shifted to the more permeable zones of the stock where the largest flow velocities occurred at approximately $t = 7 \times 10^4$ years, decreasing gradually thereafter. Fluid fluxes in the carbonate layers ranged from 10^{-8} to 10^{-9} g/cm²s at $t = 1.5 \times 10^5$ years to 10^{-7} to 10^{-8} g/cm²s at $t = 1.8 \times 10^5$ years with values, at a given time, increasing toward the stock side contact. In the shaly formations immediately above, fluid fluxes increased from an average of 5×10^{-9} g/cm²s before the first fracture event to an average of 10^{-8} g/cm²s, which persisted for most of the cooling of the stock subsequent to that event. Magnitudes of fluid fluxes varied significantly with time inside the stock. The more permeable upper half witnessed fluxes four to five orders of magnitude greater than those in the lower half, which were in the order of 10^{-12} g/cm²s. However, after the third fracture event, at $t = 6.5 \times 10^4$ years, fluid fluxes ranged from 10^{-7} to 10^{-9} g/cm²s in the upper 4 km of the stock, with values increasing with time.

The high permeabilities in the domain caused a convection-dominated system in which large amounts of fluids flowed through the heat source, thereby reducing its thermal energy to about 40 percent of the initial value after only 10^5 years of cooling. Convective heat flux at 0.25 km above the stock top reached maximum values of 11, 7, and 5 HFU at approximately 2×10^4 years after each fracture episode and was at least four times higher than the conductive heat flux during at 1.2×10^5-year period of cooling.

The heat transferred across the stock margins increased the temperature of a 1.2-km-thick pile of host rocks above the stock at an average rate of 9×10^{-3} °C/year. At approximately $t = 3 \times 10^4$ years temperatures had risen to a maximum of 350°C in those rocks which subsequently cooled at an average rate of 6×10^{-4} °C/year (Fig. 12). By $t = 1.8 \times 10^5$ years only a 0.5 km of overlying rocks was still heated above 200°C. Abundant fluid circulation into the upper stock margin and along the stock-host rock contacts inhibited a significant outward displacement of the 200°C isotherm. Inside the stock temperatures dropped very rapidly in the fractured zones (Fig. 13). The 800°C isotherm was displaced at an average rate of 12 cm/year, which was 3.5 times as high as the average displacement of the 400°C isotherm in corresponding periods of time. The upper 2 km of the stock was thus maintained at average tempera-

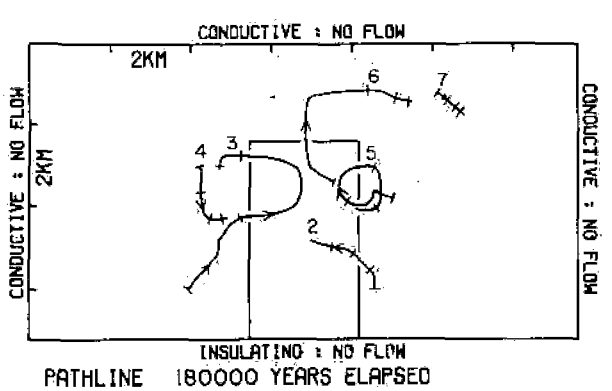

FIG. 14. Fluid pathlines in the Mayflower system representing redistribution of fluids during 1.8×10^5 years of cooling. Tick marks on path occur at $t = 0$ and every 6×10^4 years.

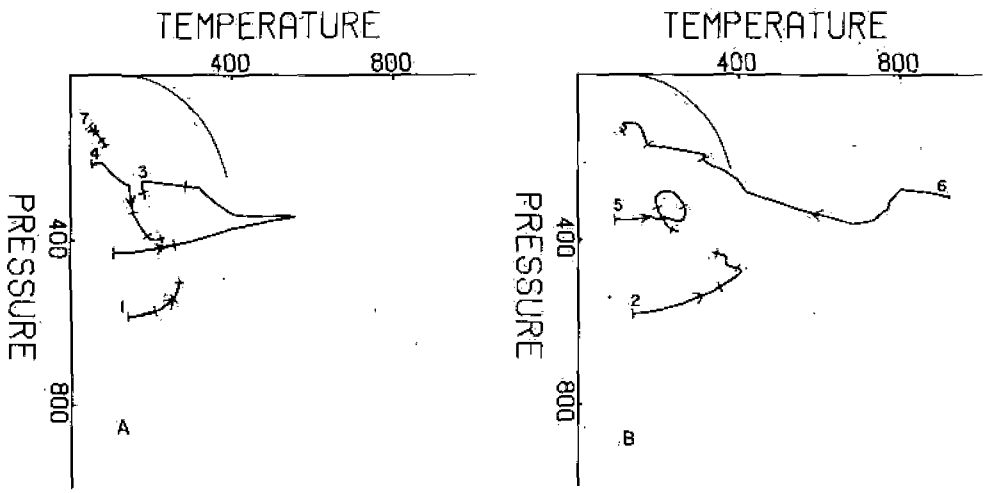

FIG. 15, A, B. Pressure-temperature conditions along pathlines in the Mayflower system, Figure 14, with respect to two-phase surface in H_2O-system. Tick marks on path occur at 6×10^4-year increments.

tures of 270°C, subsequent to the last fracture event at $t = 6.5 \times 10^4$ years, while the lower third of the stock continued to cool at a rate of 2.60×10^{-3} °C/year.

The analysis of fluid distribution in and around the Mayflower stock during its cooling provides important evidence to understanding the nature of the mineral assemblages observed in the altered rocks of have been chosen as representative of both the extent the Mayflower mine. Pathlines of seven fluid packets have been chosen as representative of both the extent to which fluids moved through contrasting chemical and mineralogical environments (Fig. 14) and the variation in pressure and temperature that those fluids experienced along their paths (Figs. 15a and 15b). Fluid packets that started in the basement rocks at different depths and distances from the stock-side contacts showed distinct pathlines during a cooling period of 1.8×10^5 years. Fluids associated with pathline 1 did not penetrate the stock, whereas those associated with pathline 2 crossed the stock margin at $t = 10^5$ years and moved 1.5 km into the stock interior. The paths of fluid packets 1 and 2 in P-T space are similar, but the fluid packets of pathline 2 were heated to higher temperatures (up to 400°C) and subjected to lower pressures (down to 425 bars). The fluid packet represented by pathline 3 crossed the stock margin at $t = 7.5 \times 10^4$ years and moved for 3 km through the stock at which point it moved to the Mesozoic shaly formation-stock contact. The fluids then circulated for over 6×10^4 years through those formations, heading toward the carbonate rocks immediately below. Along this path the temperature increased from 110° to 560°C then decreased to 180°C as fluids moved away from the stock interior. The corresponding pressure change reached a maximum of about 170 bars (Fig. 15a). The fluid packet of pathline 4, which originated in the shaly formations, moved downward through the more permeable carbonate rocks and then into the basement rocks. Both pressure and temperature increased along this path to a maximum of 400 bars and 230°C. Pathline 5 describes the path of a fluid packet residing initially in the carbonate rocks at approximately 1 km from the stock side contact. Fluids entered the stock at a depth of 4 km and moved upward inside the stock for about 1.6 km, crossing the stock-Mesozoic shale contact at approximately $t = 10^5$ years. Fluids continued to move through the shaly formations, then toward the underlying carbonate rocks to enter the stock again along the carbonate-basement rock contact at $t = 1.8 \times 10^5$ years. Fluid temperature increased isobarically to about 260°C at the stock margin, and for a period of approximately 1.4×10^5 years temperature and pressure first decreased and then increased as fluids moved out of and into the heat source. The fluid packet associated with pathline 6 crossed the upper stock contact at $t = 2 \times 10^4$ years, moving into the overlying volcanic rocks in the subsequent 1.6×10^5 years of cooling, first upward for about 1 km then laterally for about 2.5 km. The fluid packet underwent a 625°C decrease in temperature over an initial 6×10^4-year period of cooling, continuing to cool thereafter at a much slower rate. Fluid pressure increased for a short period of time, but the overall trend was a gradual decrease from 300 bars initially to 120 bars at $t = 1.8 \times 10^5$ years. Fluids represented by pathline 7, with origin in the volcanic rocks at a distance of 2.3 km from the stock upper corner, flowed only a relatively short distance and without changing pressure or temperature.

Irreversible Mass Transfer between Circulating Fluid and the Mayflower Stock

The composition and relative amounts of product minerals derived from solution-rock interactions depend upon time- and space-dependent parameters such as temperature, pressure, fluid flux, and fluid and rock compositions. The extent of alteration is measured by the distribution and abundance of alteration minerals and the gains or losses of components relative to the unaltered rock.

Mineral abundances were calculated from the chemical compositions of rocks and minerals. These data were obtained on samples collected in a region near the top of the Mayflower stock over a vertical depth of approximately 700 m and a lateral distance of about 300 m south of the Mayflower vein.

The Mayflower stock is the predominant rock unit exposed within the underground limits of the Mayflower mine. Its composition ranges from diorite to granodiorite, but it generally falls into the quartz diorite category. The Mayflower rocks are porphyritic with phenocrysts of andesine, biotite, quartz, hornblende, and K-feldspar. The groundmass is aphantic to fine grained and exhibits basically the same mineralogy. Subhedral to anhedral andesine phenocrysts show zoning, but enrichment in albite content is nonuniform toward the phenocryst edges. Andesine is the most abundant phenocryst and is the major component of the groundmass. The most common alteration products replacing andesine are kaolinite, sericite, epidote, calcite, anhydrite, and chlorite.

Biotite is present in varying amounts and constitutes the second most abundant phenocryst in the rocks. In the groundmass it occurs as scattered flakes less than 0.5 mm in length. In some instances biotite is found replacing hornblende. Most samples contain clusters of fine-grained biotite, about 0.1 mm long, apparently the result of alteration of earlier biotite phenocrysts. The most common alteration products of biotite are chlorite, epidote, fine-grained calcite, and sphene.

Hornblende has an occurrence similar to that of the biotite with which it is usually associated. Generally, it is present as an accessory mineral, although in a few cases it comprises up to 15 percent of the rock volume. It appears usually in subhedral crystals, commonly altered to chlorite.

Quartz exists both as phenocrysts and small grains in varying amounts and has been introduced along with the veinlets that transect the rock. In general, it forms small anhedral equant crystals, especially in the groundmass.

K-feldspar occurs rarely as phenocrysts. When present, it shows anhedral crystals of orthoclase or microcline slightly altered to kaolinite or sericite. In the groundmass it is more abundant, especially as a hydrothermal alteration product. Augite, apatite, sphene, and zircon occur as accessories.

The Ontario stock is exposed only on the 2,800-ft and 3,000-ft levels of the Mayflower mine. The Ontario rocks are porphyritic, although some facies are nearly equigranular, and their composition ranges from quartz monzonite to quartz diorite. Petrographically, the Mayflower and Ontario stocks look alike; their minerals display essentially the same textural characteristics, except that some plagioclase phenocrysts in the Ontario rocks have a myrmekitic intergrowth of quartz.

The Valeo porphyry rocks are exposed in the west side of the mine between the 800-ft and 1,270-ft levels, forming a thick sill-like body between sedimentary walls. It reappears on the 2,005-ft level as small dikes or tongue-shaped intrusions cutting through calcareous units. These rocks have a distinctive porphyritic texture with phenocrysts of oligoclase-andesine and quartz (some with rounded outlines) embedded in a fine-grained groundmass. Plagioclase phenocrysts are tabular, reaching up to 1 cm in length. Mafic minerals, particularly biotite, are present as scattered small crystals but are not abundant. K-feldspar occurs in larger amounts than in the other two stocks, and some grains are perthitic. Pyrite, kaolinite, sericite, calcite, and chlorite are the principal alteration minerals found in the Valeo stock.

The chemical and mineral compositions of the igneous rocks were quantitatively determined on samples representing a depth of about 670 m (between the 800-ft and the 3,000-ft levels), and a lateral distance of 2.0 km along drifts and crosscuts was examined, of which 1.4 km was sampled along north-south directions. The remaining 0.6 km was mapped in laterals parallel to the Mayflower-Pearl system along east-northeast–west-southwest directions. Observations were made and samples collected over 15-m intervals or less. Continuous rock chip samples covered the whole extension of each interval; a few were restricted to the immediate vicinity of veins. In addition, 305 m of core samples from a vertical diamond drill hole located near the shaft on the 3,000-ft level were studied.

One hundred and thirty samples were chemically analyzed for all major components except chemically bound water (Table 2). Si, Al, Fe (total iron as Fe^{2+}), Mg, Ca, Na, K, Mn, and Ti were determined by X-ray fluorescence spectroscopy, whereas sulfur (both sulfide and sulfate) was determined with a LECO automatic titrator. Carbon dioxide was determined with a selective collecting-gas system adapted to a LECO induction furnace (cf. Villas, 1975, for analytical procedures).

TABLE 2. Grain and Bulk Densities, Porosity, and Bulk Chemical Composition of the Igneous Rocks of the Mayflower Mine

	G/CM**3		PER CENT	WEIGHT PER CENT											
SAMPLE	GRDENS	BKDENS	PRSTY	SIO2	AL2O3	FEO	MGO	CAO	NA2O	K2O	S	CO2	MNO	SO3	TIO2	TOTAL
MF-0801	2.821	2.78	1.45	58.20	16.70	4.25	3.61	5.60	3.67	3.27	0.58	1.32	0.15	0.19	0.86	98.40
MF-0802	2.819	2.79	1.03	54.40	17.40	4.85	4.18	7.01	3.30	2.77	0.93	1.87	0.20	0.22	0.95	98.08
MF-0803	2.849	2.74	3.83	56.50	17.60	4.43	4.31	6.08	3.56	2.55	0.34	1.21	0.13	0.22	0.95	97.88
MF-0804	2.885	2.75	4.68	57.00	18.00	4.97	3.90	5.97	3.62	2.61	0.81	1.49	0.12	0.00	0.93	99.42
MF-1301	2.761	2.70	2.21	61.50	17.20	3.67	2.50	4.74	3.27	3.62	0.47	1.31	0.17	0.02	0.69	99.16
MF-1302	2.785	2.73	1.97	61.50	17.20	3.89	2.50	4.00	3.16	3.72	0.41	0.70	0.29	0.00	0.71	98.08
MF-1303	2.754	2.70	1.96	61.50	15.30	3.92	2.30	4.04	2.87	3.43	1.74	1.07	0.35	1.02	0.53	98.07
MF-1304	2.759	2.73	1.05	61.70	17.20	4.18	2.77	3.81	3.03	3.92	0.84	0.66	0.30	0.11	0.74	99.26
MF-1306	2.827	2.70	4.49	59.10	16.70	4.00	2.52	5.62	3.58	2.95	0.60	1.12	0.10	0.35	0.73	97.37
MF-1501	2.811	2.78	1.10	60.40	17.10	3.72	2.78	4.87	3.10	3.15	0.20	1.19	0.11	0.16	0.72	97.50
MF-1502	2.825	2.75	2.65	59.70	16.80	3.78	2.71	4.53	3.24	3.05	1.22	1.04	0.12	0.00	0.66	96.85
MF-1503	2.746	2.71	1.31	60.30	16.50	3.82	2.79	3.92	3.10	3.33	0.81	0.89	0.38	0.17	0.62	96.63
MF-1504	2.759	2.72	1.41	61.50	16.20	4.14	2.72	3.93	2.98	3.65	0.85	0.90	0.33	0.15	0.67	98.02
MF-1505	2.821	2.75	2.52	59.40	17.50	4.40	3.32	5.36	3.52	3.05	0.24	0.42	0.10	0.13	0.94	98.38
MF-1506	2.681	2.61	2.65	43.50	13.50	4.59	1.74	19.74	1.44	2.34	1.11	9.81	0.38	2.17	0.48	100.80
MF-1701V	2.765	2.72	1.63	56.90	13.30	7.53	1.74	4.42	1.90	2.55	6.18	2.52	0.39	1.49	0.49	99.41
MF-1702	2.795	2.76	1.25	58.20	16.80	5.16	3.39	3.68	2.41	4.30	1.40	0.97	0.51	0.33	0.80	97.95
MF-1703	2.755	2.72	1.27	57.40	17.80	4.36	3.37	4.76	3.24	3.44	0.27	1.03	0.23	0.67	0.83	97.40
MF-1704	2.780	2.74	1.44	58.80	17.90	4.27	3.60	4.74	3.36	3.37	0.40	0.72	0.19	0.20	0.83	98.38
MF-1705	2.777	2.74	1.33	58.30	17.30	4.44	3.52	4.52	2.96	3.69	0.49	0.67	0.35	0.33	0.77	97.34
MF-1706	2.750	2.71	1.45	54.70	16.50	4.10	2.89	7.80	2.53	3.49	1.74	4.77	0.26	0.00	0.57	99.35
MF-1707	2.798	2.75	1.72	56.70	17.50	4.29	3.39	6.20	3.04	3.09	0.43	1.66	0.24	0.30	0.82	97.66
MF-1708	2.794	2.74	1.93	55.00	15.90	4.22	3.23	7.79	2.79	2.84	0.82	2.67	0.21	0.75	0.78	97.00
MF-1709	2.784	2.73	1.94	57.50	17.20	4.39	3.45	6.06	3.27	2.96	0.22	0.96	0.13	0.24	0.85	97.23

TABLE 2—(*Continued*)

	G/CM**3		PER CENT	WEIGHT PER CENT												
SAMPLE	GRDENS	BKDENS	PRSTY	SIO2	AL2O3	FEO	MGO	CAO	NA2O	K2O	S	CO2	MNO	SO3	TIO2	TOTAL
MF-1710	2.774	2.76	0.50	58.70	16.90	4.45	3.60	5.18	3.21	3.03	0.49	0.69	0.12	0.01	0.84	97.22
MF-1711	2.791	2.72	2.54	61.60	17.70	4.26	2.96	4.90	3.79	3.25	0.27	0.40	0.10	0.17	0.82	100.22
MF-1712	2.735	2.71	0.91	58.90	17.20	4.34	3.17	5.83	3.41	2.99	0.98	1.74	0.10	0.11	0.77	99.54
VL-2001	2.733	2.70	1.21	63.00	17.70	1.96	2.70	2.48	2.70	6.01	1.09	0.96	0.16	0.00	0.45	99.21
VL-2002	2.664	2.59	2.78	62.10	18.40	2.02	3.54	2.20	2.33	6.07	1.34	.84	.14	0.00	.46	99.44
MF-2001	2.793	2.67	4.40	59.10	18.10	3.47	2.71	4.10	3.04	3.57	0.96	1.25	0.15	0.84	0.64	97.93
MF-2002	2.834	2.77	2.26	60.20	18.00	3.53	2.36	3.58	3.07	3.82	1.43	1.09	0.16	0.13	0.59	97.96
MF-2003	2.788	2.74	1.72	53.60	16.80	5.03	4.36	6.50	2.16	3.61	1.38	2.76	0.65	0.48	0.64	97.97
MF-2004	2.687	2.59	3.61	58.10	17.30	4.97	3.86	3.16	2.16	3.86	1.47	1.15	0.52	0.42	0.74	97.71
MF-2005	2.774	2.74	1.23	61.30	17.50	3.89	3.42	3.68	3.70	3.25	0.90	0.60	0.12	0.46	0.72	99.54
MF-2006	2.868	2.76	3.77	55.70	17.20	4.91	4.88	5.22	3.24	2.74	0.66	0.40	0.10	1.14	1.00	97.19
MF-2007	2.836	2.76	2.68	53.58	17.40	4.87	4.53	6.36	3.04	2.88	1.00	0.75	0.08	2.58	0.92	97.99
MF-2008	2.798	2.78	0.64	53.66	16.80	4.75	4.32	6.31	3.01	2.61	1.08	0.68	0.06	2.51	0.87	96.66
MF-2009	2.797	2.74	2.04	51.43	16.00	3.91	4.17	8.26	2.76	2.18	2.28	1.11	0.09	3.86	0.60	96.65
MF-2010	2.744	2.73	0.51	52.36	16.20	4.89	4.67	6.96	2.84	2.42	2.82	1.45	0.06	3.18	0.64	98.49
MF-2011	2.824	2.74	2.97	59.20	16.70	4.96	3.15	3.69	2.41	3.70	1.37	1.30	0.72	0.00	0.72	97.92
MF-2012	2.751	2.73	0.76	60.17	15.50	4.98	2.90	3.92	1.93	3.70	2.27	1.70	0.63	0.89	0.60	99.19
MF-2013	2.798	2.74	2.07	58.40	17.50	4.34	3.29	5.36	3.65	3.19	0.24	0.64	0.15	0.40	0.76	97.92
MF-2014	2.764	2.72	1.59	57.90	16.90	4.07	3.43	5.17	3.06	3.66	0.73	1.12	0.25	0.35	0.76	97.40
MF-2015	2.854	2.76	3.29	58.10	17.60	4.34	4.11	5.73	3.21	2.94	0.28	0.87	0.15	0.00	0.90	98.23
MF-2016	2.782	2.73	1.87	59.50	17.50	4.28	4.04	5.79	3.21	2.98	0.16	0.97	0.12	0.67	0.89	100.11
MF-2017	2.777	2.71	2.41	59.50	18.00	4.27	3.43	6.14	3.35	3.08	0.22	1.32	0.12	0.00	0.88	100.31
MF-2018	2.822	2.75	2.55	61.10	18.20	3.93	3.04	5.10	3.94	2.95	0.12	0.48	0.10	0.58	0.82	100.36
MF-2001				59.90	16.80	3.10	2.08	4.65	2.19	3.80	1.49	2.10	0.34	.76	.49	97.70

TABLE 2—(*Continued*)

	G/CM**3		PER CENT	WEIGHT PER CENT											
SAMPLE	GRDENS	BKDENS	PRSTY	SIO2	AL203	FEO	MGO	CAO	NA2O	K2O	S	CO2	MNO	SO3	TIO2	TOTAL
MF-2202	2.761	2.65	4.02	62.48	18.27	3.00	3.00	3.38	3.79	3.11	0.80	0.53	0.08	0.65	0.60	99.69
MF-2203	2.784	2.64	5.17	59.93	17.30	5.19	4.07	4.06	4.16	3.31	1.48	0.50	0.12	1.24	0.79	99.16
MF-2004				59.10	18.40	4.52	4.64	4.37	4.08	2.51	0.53	0.70	0.18	0.42	0.76	100.31
MF-2205	2.781	2.71	2.55	55.70	17.60	5.16	4.85	4.91	2.77	3.25	1.25	0.83	0.31	0.87	0.74	98.24
MF-2206	2.800	2.74	2.14	57.10	18.00	4.51	3.79	5.72	4.16	2.40	0.57	0.57	0.07	2.02	0.75	99.66
MF-2207	2.753	2.72	1.20	57.40	17.80	4.30	3.49	5.78	3.76	2.69	0.64	0.54	0.07	2.04	0.81	99.32
MF-2208	2.793	2.76	1.18	56.60	16.30	4.26	3.54	6.56	3.06	2.36	1.00	0.77	0.10	3.10	0.67	98.32
MF-2209	2.894	2.85	1.52	53.54	15.30	3.97	4.61	9.44	2.92	1.71	1.09	1.95	0.07	4.59	0.56	99.75
MF-2210	2.772	2.70	2.60	54.90	17.20	4.96	4.32	6.94	3.57	2.47	0.59	1.00	0.10	0.79	0.96	97.80
MF-2211	2.766	2.64	4.56	54.40	17.30	4.81	4.46	7.97	3.43	1.91	0.60	0.53	0.12	0.71	1.04	97.28
MF-2212	2.760	2.75	0.36	57.10	18.00	4.64	4.14	6.11	4.45	2.70	0.27	0.45	0.12	0.32	0.98	99.28
MF-2213	2.801	2.77	1.11	55.80	17.40	4.99	4.43	6.70	3.36	2.75	0.23	0.76	0.12	0.38	1.00	97.92
MF-2214	2.778	2.72	2.09	56.60	17.30	5.23	4.36	6.12	3.36	2.95	0.44	0.84	0.14	0.06	1.08	98.48
MF-2601	2.727	2.63	3.56	60.70	17.46	4.95	3.11	3.18	3.43	2.90	2.48	0.45	0.05	0.51	0.66	99.88
MF-2602	2.709	2.61	3.65	60.90	17.95	4.36	3.15	3.19	3.94	2.61	2.03	0.49	0.35	0.34	0.67	99.98
MF-2603	2.824	2.74	2.97	60.10	17.57	5.38	3.15	3.17	3.57	2.62	2.70	0.36	0.05	0.79	0.68	100.14
MF-2604	2.834	2.72	4.02	60.03	16.99	5.37	3.40	3.85	3.58	2.62	2.67	0.37	0.05	1.20	0.65	100.78
MF-2605	2.785	2.72	2.33	57.60	17.00	5.32	3.23	4.34	3.79	2.70	2.67	0.53	0.07	1.20	0.62	99.07
MF-2606	2.755	2.69	2.36	59.23	17.09	4.63	3.11	4.13	3.79	2.91	2.24	0.47	0.05	1.52	0.63	99.80
MF-2607	2.775	2.72	1.98	59.10	17.18	5.08	3.47	3.56	3.14	2.49	2.47	0.69	0.05	2.07	0.69	99.99
MF-2608	2.776	2.72	2.02	60.10	16.51	4.60	4.11	3.91	3.21	2.88	2.05	0.28	0.05	1.14	0.75	99.59
MF-2609	2.813	2.71	3.66	60.06	16.69	5.46	3.96	2.94	3.14	3.04	2.62	0.36	0.06	0.39	0.73	99.45
MF-2610	2.801	2.63	6.10	58.10	17.20	6.61	3.38	3.20	3.00	3.45	3.43	0.35	0.05	0.89	0.82	100.48
MF-2611	2.782	2.66	4.39	59.17	17.41	5.93	4.39	2.65	3.21	2.88	2.48	0.49	0.06	0.70	0.74	100.11

TABLE 2—(*Continued*)

	G/CM**3		PER CENT	WEIGHT PER CENT											
SAMPLE	GRDENS	BKDENS	PRSTY	SIO2	AL2O3	FEO	MGO	CAO	NA2O	K2O	S	CO2	MNO	SO3	TIO2	TOTAL
MF-2612	2.779	2.75	1.04	59.57	16.64	5.82	3.72	3.29	3.94	2.54	2.27	0.23	0.05	1.10	0.72	99.89
MF-2613	2.756	2.72	1.31	57.74	16.12	5.39	3.47	5.51	3.53	2.69	2.40	0.57	0.04	2.90	0.64	101.00
MF-2614	2.782	2.74	1.51	58.88	16.18	4.66	2.90	4.89	3.72	3.13	2.00	0.43	0.04	2.90	0.64	100.37
MF-2615	2.832	2.75	2.90	55.80	16.30	5.30	3.47	6.00	3.65	2.90	2.27	0.40	0.04	3.19	0.63	99.95
MF-2616	2.765	2.75	0.54	57.50	17.50	4.73	3.29	5.07	3.57	2.88	1.98	0.33	0.04	2.62	0.66	100.17
MF-2617	2.835	2.78	1.94	59.85	16.99	4.13	3.43	4.41	3.94	2.99	1.24	0.63	0.05	1.67	0.68	100.01
MF-2618	2.727	2.64	3.19	62.90	17.95	3.07	2.04	3.73	3.50	3.55	0.64	0.42	0.06	1.10	0.57	98.54
MF-2619	2.768	2.62	5.35	61.25	17.66	4.55	2.65	3.18	2.99	3.52	1.50	0.47	0.09	0.71	0.63	99.20
MF-2620	2.811	2.69	4.30	60.45	17.02	4.49	2.53	3.95	3.35	3.66	1.33	0.58	0.11	1.33	0.61	99.41
MF-2621	2.811	2.79	0.74	61.10	17.10	4.06	2.29	4.08	3.21	3.29	1.75	0.38	0.07	1.72	0.54	99.59
MF-2622	2.742	2.69	1.90	61.40	17.20	2.93	2.22	4.58	3.86	3.10	0.75	0.36	0.08	0.86	0.58	97.92
MF-2623	2.728	2.70	1.03	60.55	17.55	4.00	2.72	4.29	4.37	2.49	1.30	0.45	0.06	1.52	0.56	99.86
MF-2624	2.735	2.63	3.84	58.50	16.90	3.01	2.61	5.84	3.14	2.00	0.90	0.64	0.10	3.39	0.56	98.39
MF-2625	2.724	2.70	0.88	61.60	18.00	3.14	2.11	4.53	3.79	3.06	0.82	0.57	0.08	1.50	0.55	99.75
MF-2626	2.830	2.73	3.53	54.80	16.90	4.22	2.90	6.60	4.01	2.46	1.22	0.47	0.06	3.63	0.66	97.93
MF-2627	2.797	2.72	2.75	61.70	17.40	3.07	1.65	5.11	2.99	3.40	1.28	1.18	0.11	2.21	0.54	100.64
MF-2628	2.753	2.65	3.95	62.10	17.80	3.12	1.97	3.96	2.55	3.98	1.34	0.83	0.14	1.86	0.51	100.16
MF-2629	2.755	2.74	0.54	56.30	15.90	3.03	2.79	7.02	2.84	3.24	1.06	1.33	0.05	5.43	0.59	99.58
MF-2630	2.797	2.74	2.04	59.86	16.79	4.52	3.34	4.04	2.74	3.50	2.10	1.52	0.17	0.46	0.72	99.76
MF-2631	2.769	2.75	0.69	55.70	17.70	3.82	3.15	6.28	3.50	2.44	1.03	0.83	0.05	2.83	0.80	98.13
MF-2632	2.787	2.76	0.97	56.30	17.60	3.60	2.76	6.25	3.57	2.75	1.17	0.64	0.11	2.80	0.70	98.25
MF-2633	2.824	2.76	2.27	55.10	17.40	3.95	3.97	7.12	3.28	2.73	1.06	1.06	0.10	1.76	0.87	98.40
MF-2634	2.804	2.78	0.86	53.30	17.30	5.29	4.61	6.03	2.29	2.65	2.51	0.67	0.06	2.37	0.86	97.94
MF-2801	2.782	2.72	2.23	54.21	17.65	5.34	2.75	5.28	1.68	4.13	2.84	2.13	0.34	1.80	0.53	98.68

TABLE 2—(*Continued*)

	G/CM**3		PER CENT	WEIGHT PER CENT											
SAMPLE	GRDENS	BKDENS	PRSTY	SIO2	AL2O3	FEO	MGO	CAO	NA2O	K2O	S	CO2	MNO	SO3	TIO2	TOTAL
MF-2802	2.790	2.70	3.23	59.30	17.10	3.43	2.83	4.75	2.92	2.91	1.28	0.66	0.06	2.06	0.66	97.96
MF-2803	2.813	2.75	2.24	56.60	16.50	3.98	3.40	5.91	3.21	2.79	1.49	0.66	0.06	3.90	0.60	99.10
MF-2804	2.819	2.78	1.38	56.20	17.20	4.92	4.75	5.59	3.87	2.61	2.53	0.60	0.04	1.93	0.80	101.04
MF-2805	2.799	2.76	1.39	51.70	15.70	6.85	4.33	6.67	2.97	2.78	3.79	1.77	0.24	1.87	0.80	99.47
MF-2806	2.829	2.78	1.73	55.50	16.40	5.51	4.61	5.91	2.92	2.49	2.07	0.62	0.06	2.42	0.74	99.25
MF-2807	2.822	2.76	2.20	56.80	16.32	4.86	5.25	5.63	3.14	2.83	1.39	1.32	0.06	2.57	0.79	100.96
MF-2808	2.775	2.76	0.54	56.20	15.90	5.38	4.50	5.57	3.06	2.55	2.84	0.66	0.07	1.79	0.73	99.25
MF-2809	2.789	2.67	4.27	55.16	16.00	5.54	5.28	5.61	3.21	2.57	2.13	0.56	0.11	2.78	0.81	99.76
MF-2810	2.811	2.78	1.10	52.60	14.90	7.06	4.85	6.17	2.72	2.81	3.85	0.90	0.11	2.77	0.83	99.57
MF-2811	2.794	2.76	1.22	55.70	15.90	5.63	5.89	5.89	3.28	2.39	1.48	0.61	0.06	1.85	0.88	99.56
ON-2801	2.754	2.70	1.96	61.30	17.50	3.25	2.36	4.24	3.21	3.94	1.32	0.77	0.12	1.76	0.57	100.34
ON-2802	2.697	2.63	2.48	62.30	18.30	3.30	2.26	2.96	3.43	3.70	1.36	0.43	0.05	0.90	0.59	99.58
ON-2804	2.927	2.84	2.97	59.60	17.60	5.63	2.90	2.69	2.55	3.62	2.94	0.38	0.12	0.82	0.59	99.44
MF-3001	2.845	2.76	2.99	55.32	16.00	5.45	4.06	5.53	3.52	2.81	2.12	0.28	0.05	2.50	0.77	98.41
MF-3002	2.808	2.77	1.35	56.86	16.14	4.93	4.04	5.70	3.72	2.57	1.79	0.33	0.05	1.40	0.76	98.29
MF-3003	2.817	2.74	2.73	54.90	14.90	6.07	4.16	5.68	3.38	2.87	2.84	0.43	0.05	2.62	0.74	98.64
MF-3004	2.815	2.75	2.31	55.80	15.40	5.16	4.16	5.82	3.55	2.52	1.62	1.20	0.05	2.59	0.75	98.62
MF-3005	2.873	2.78	3.24	54.70	14.80	6.23	3.96	5.70	3.43	2.80	3.24	0.48	0.09	2.80	0.69	98.92
MF-3006	2.771	2.74	1.12	54.90	15.40	5.92	4.89	6.43	3.38	2.47	1.36	0.40	0.06	2.85	0.79	98.85
MF-3007	2.792	2.75	1.50	52.70	15.60	6.91	5.38	5.98	3.18	2.54	3.54	0.70	0.10	2.00	0.80	99.43
MF-3008	2.795	2.77	0.89	53.70	16.50	5.65	5.66	5.83	2.81	3.04	1.64	0.59	0.10	2.12	0.94	98.58
MF-3009	2.822	2.76	2.20	53.90	17.10	5.78	5.84	6.07	3.33	2.78	1.78	0.52	0.09	1.53	0.89	99.61
ON-3001	2.882	2.79	3.19	58.90	17.70	4.56	2.95	4.49	3.36	3.26	1.81	0.46	0.09	0.41	0.63	98.62
ON-3002	2.785	2.68	3.77	60.60	17.20	3.32	2.52	4.27	3.41	3.55	1.14	0.51	0.06	1.25	0.58	98.41

TABLE 2—(*Continued*)

	G/CM**3		PER CENT	WEIGHT PER CENT											
SAMPLE	GRDENS	BKDENS	PRSTY	SIO2	AL2O3	FEO	MGO	CAO	NA2O	K2O	S	CO2	MNO	SO3	TIO2	TOTAL
ON-3003	2.769	2.70	2.49	61.70	16.90	3.21	2.24	4.21	2.71	4.44	1.27	1.04	0.13	0.90	0.59	99.34
ON-3004	2.834	2.76	2.61	60.70	16.70	3.20	2.24	4.52	3.06	4.32	1.66	1.16	0.17	1.77	0.55	100.05
ON-3005	2.750	2.69	2.18	59.80	18.10	3.91	2.25	3.75	2.33	5.17	2.24	1.19	0.14	0.27	0.58	99.73
ON-3005V				58.10	17.60	4.59	2.31	3.08	2.02	5.04	3.27	1.29	0.18	1.22	0.58	99.28
ON-3006	2.776	2.72	2.02	59.50	16.80	3.45	2.71	4.55	3.47	4.07	1.15	0.56	0.10	1.88	0.53	98.77
ON-3007	2.753	2.72	1.20	57.90	17.30	5.28	3.32	4.25	2.13	3.74	2.00	1.06	0.35	1.36	0.59	99.28
DDH-216	2.794	2.78	0.50	55.80	16.10	4.09	5.35	6.35	4.23	2.45	0.50	0.38	0.06	2.95	0.80	99.06
DDH-350	2.803	2.78	0.82	56.20	16.60	4.23	5.03	6.06	3.72	2.75	0.77	0.36	0.08	1.14	0.83	97.77
DDH-639	2.753	2.70	1.93	62.00	17.30	2.86	2.26	4.38	4.37	2.54	0.28	0.33	0.05	1.36	0.60	98.33
DDH-770	2.747	2.70	1.71	62.10	17.20	3.34	1.33	3.33	3.59	3.34	1.26	0.35	0.04	1.39	0.49	97.76
DDH-992	2.856	2.77	3.01	55.10	16.40	5.31	5.10	6.05	3.21	2.64	1.16	0.30	0.05	3.53	0.78	99.63

TABLE 3. Estimated Composition of the Unaltered Mayflower and Ontario Stocks

	Mayflower[1]		Ontario
	Calculated	MF-2018†	
	Weight percent.		
SiO_2	59.40	61.10	60.80
Al_2O_3	20.60	18.20	16.70
FeO	4.30*	3.93	1.20
Fe_2O_3	—	—	3.96
MgO	1.90	3.04	1.81
CaO	5.90	5.10	3.15
Na_2O	4.90	3.94	5.39
K_2O	2.10	2.95	3.60
S	—	0.12	3.60
H_2O†	0.45	—	0.73
H_2O	—	—	0.44
CO_2	—	0.48	—
SO_3	—	0.58	—
MnO	0.05	0.10	—
TiO_2	0.40	0.10	—
Total	100.00	100.36	97.80
Bulk density	2.69	2.75	

[1] Villas, 1975.
† Least altered Mayflower rock sampled.
* Total iron as FeO.

Unaltered specimens of igneous rocks were not found in the mine. Therefore, estimates of their original chemical compositions became necessary to determine the extent to which hydrothermal fluids reacted with the igneous rocks.

Chemical compositions of the unaltered Mayflower rocks were, on the other hand, approximated from modal analysis of the least altered samples and from the chemical compositions of primary minerals, with the exception of igneous biotite. Mineral modes for the unaltered rocks were estimated as follows: andesine, 69 ± 5 percent; orthoclase, 5 ± 2 percent; quartz, 10 ± 3 percent; biotite, 12 ± 3 percent; hornblende, 3 ± 1 percent; and magnetite, 1 ± 0.5 percent. The corresponding calculated chemical composition is given in Table 3. Iron was assumed to be conserved in the system, implying that iron-bearing alteration phases were primarily formed with iron derived from the dissolution of igneous mafic minerals and magnetite. Because the mole fraction, N, of annite and phlogopite in present-day biotite ($N_{ann} = 0.36$ and $N_{phl} = 0.64$) would fall short of accounting for the observed amounts of iron in the altered Mayflower rocks, the igneous biotite was assumed to correspond to 7 weight percent annite and 5 weight percent phlogopite. These values fix the igneous biotite composition, making it equivalent to the member of the biotite solid solution series characterized by 58 weight percent annite and 42 weight percent phlogopite (or $N_{ann} = 0.53$ and $N_{phl} = 0.47$). The more magnesian character found for hydrothermal biotites in other areas (Beane, 1974; Jacobs and Parry, 1976) adds qualitative evidence to support these assumptions.

Mineral Assemblages

Andesine, quartz, orthoclase, biotite, and hornblende are the major primary minerals of the unaltered counterparts of the stocks exposed in the Mayflower mine. The alteration assemblages of these stocks; on the other hand, are much more varied, but only a few minerals occur in significant quantities over the studied vertical section of the mine. The most abundant alteration products are kaolinite, K-feldspar, quartz, biotite, chlorite, anhydrite, calcite, and pyrite. Minor alteration components include actinolite, epidote, salite, zeolite, rhodochrosite, schorlite, and magnetite, which locally are abundant, especially as vein-filling minerals. Sericite, although ubiquitous, is not abundant except locally in the immediate vicinity of the main vein system. Albite, likewise, is not widespread but is a major hydrothermal mineral in the range of two to five meters from the Mayflower vein. Montmorillonite was not found in this study, but it has been reported to occur ubiquitously in small amounts above the 800-ft level (Williams, 1952).

Chemical Compositions of the Mineral Phases

Only silicate minerals that usually exhibit significant compositional variation, e.g., members of solid solution series, were analyzed. Grains of biotite, chlorite, hornblende, actinolite, epidote, salite, augite, plagioclase, and K-feldspar in carbon-coated polished thin sections were examined with an electron microprobe. Chemical determinations were made for nine major elements, Si, Al, Fe (total iron as Fe^{2+}), Mg, Ca, Na, K, Ti, and Mn (Table 4). Biotite analyses also include F, Cl, and Ba, while Ca, Na, and K were the only elements determined in feldspar grains. Eighteen microprobe sections were prepared from samples collected in all levels of the mine studied. As a rule, mineral compositions determined from a mount were taken as representative for the level from which the sample came. On levels where more than one sample was analyzed, determined mineral compositions were assigned to the intervals closest to the sampling site. The minerals analyzed show remarkably uniform compositions despite their spatial distribution in the cross section of the mine and their mode of occurrence.

Mineral Abundance Determinations

The relative amounts of reactant and product minerals composing the igneous rocks of the Mayflower mine were calculated using a least squares regression

TABLE 4. Structural Formulas of Minerals Used in Mass Abundance Calculations, Mayflower, Ontario, and Valeo Stocks

MINERAL	GRAM . ATOM / MOLE											
	SI	AL	FE	MG	CA	NA	K	MN	TI	RA	O	H2O
ANALYSED WITH THE ELECTRON MICROPROBE												
BIOTITE												
MF-0801	2.84	1.13	0.96	1.56	0.01	0.04	0.84	0.02	0.29	0.05	11.0	1.0
MF-1306	2.89	1.10	0.97	1.73	0.01	0.03	0.88	0.02	0.20	0.01	11.0	1.0
MF-1504	2.81	1.21	0.92	1.75	0.01	0.03	0.86	0.02	0.20	0.02	11.0	1.0
MF-1708	2.90	1.09	0.95	1.71		0.02	0.90	0.01	0.21		11.0	1.0
MF-2011	2.84	1.18	0.93	1.77		0.04	0.80	0.01	0.21	0.01	11.0	1.0
MF-2201	2.85	1.23	0.90	1.60	0.01	0.04	0.85	0.01	0.23	0.02	11.0	1.0
MF-2204	2.88	1.09	0.96	1.78	0.01	0.04	0.87	0.01	0.19	0.01	11.0	1.0
MF-2206	2.90	1.10	0.97	1.71	0.01	0.03	0.87	0.02	0.19	0.01	11.0	1.0
MF-2211	2.83	1.18	1.01	1.54	0.02	0.04	0.89	0.02	0.23	0.04	11.0	1.0
MF-2603	2.77	1.30	1.20	1.53	0.01	0.05	0.87	0.02	0.21	0.03	11.0	1.0
MF-2634	2.79	1.18	0.87	1.85	0.02	0.04	0.86	0.01	0.21	0.01	11.0	1.0
MF-2802	2.84	1.21	0.86	1.58	0.04	0.04	0.86		0.29	0.01	11.0	1.0
MF-3005	2.83	1.18	1.02	1.59	0.01	0.04	0.92	0.01	0.22	0.02	11.0	1.0
DDH-177	2.80	1.20	0.79	2.00	0.02	0.03	0.84	0.01	0.17	0.01	11.0	1.0
DDH-812	2.79	1.26	0.99	1.64		0.05	0.87	0.01	0.20	0.02	11.0	1.0
ON-3005	2.74	1.28	0.97	1.66		0.04	0.88	0.01	0.24	0.02	11.0	1.0
VL-2002	2.73	1.29	0.36	2.51		0.02	0.84	0.01	0.14		11.0	1.0
CHLORITE												
MF-0801	5.87	4.20	3.29	6.51	0.05	0.04		0.07	0.01		28.0	8.0
MF-0801V	5.84	4.25	2.91	6.91	0.03	0.05		0.06			28.0	8.0
MF-0804	5.80	4.08	2.59	7.54	0.03	0.05		0.08	0.01		28.0	8.0
MF-1306	5.70	4.21	3.36	6.77	0.03	0.04		0.08	0.01		28.0	8.0
MF-1504	5.73	4.13	3.22	6.97	0.02	0.04	0.01	0.04	0.02		28.0	8.0
MF-1708	5.77	4.13	3.41	6.63	0.02	0.02	0.03	0.07	0.01		28.0	8.0
MF-2011	5.76	4.20	3.48	6.59	0.03	0.04	0.01	0.04	0.08		28.0	8.0
MF-2201	5.83	4.46	3.58	5.86	0.02	0.01	0.01	0.17	0.01		28.0	8.0
MF-2204	5.89	4.06	3.45	6.52	0.04	0.06	0.01	0.07	0.01		28.0	8.0
MF-2206	5.73	4.13	3.53	6.61	0.02	0.02	0.02	0.13	0.01		28.0	8.0
MF-2211	5.82	4.18	3.54	6.37	0.06	0.04	0.01	0.07	0.01		28.0	8.0
MF-2603	5.58	4.46	3.01	7.05	0.02	0.04	0.01	0.06			28.0	8.0
MF-2634	5.74	4.20	3.55	6.54	0.05	0.04		0.05	0.01		28.0	8.0
MF-2802	5.74	4.30	3.56	6.43	0.02	0.02		0.02	0.01		28.0	8.0
MF-3005	5.85	4.23	3.66	6.19	0.04	0.05	0.04	0.05	0.01		28.0	8.0
DDH-177	5.85	4.02	3.53	6.62	0.04	0.03	0.02	0.04	0.01		28.0	8.0
DDH-177V	5.86	4.04	4.01	6.10	0.07	0.01		0.05			28.0	8.0

TABLE 4—(*Continued*)

	SI	AL	FE	ME	CA	NA	K	MN	TI	RA	O	H2O
DDH-812	5.48	4.42	3.48	6.80	0.02	0.03	0.01	0.06	0.01		28.0	8.0
ON-3005	5.51	4.39	3.74	6.55	0.02	0.01	0.02	0.05	0.01		28.0	8.0
VL-2002	5.54	4.15	1.75	8.39	0.01	0.02	0.02	0.17	0.01		28.0	8.0
ACTINOLITE												
MF-0801	7.79	0.39	1.24	3.55	1.87	0.10	0.02	0.08	0.02		23.0	1.0
MF-1306	7.40	0.89	1.65	3.01	1.78	0.24	0.09	0.07	0.10		23.0	1.0
MF-2011	7.51	0.76	1.33	3.47	1.77	0.18	0.07	0.04	0.04		23.0	1.0
MF-2204	7.49	0.62	1.46	3.49	1.91	0.17	0.05	0.04	0.04		23.0	1.0
MF-2206	7.61	0.65	1.37	3.39	1.82	0.16	0.05	0.07	0.03		23.0	1.0
MF-2211	7.41	0.75	1.50	3.28	1.72	0.22	0.07	0.07	0.11		23.0	1.0
MF-2634	7.60	0.52	1.55	3.39	1.97	0.09	0.03	0.03	0.01		23.0	1.0
MF-3005	7.71	0.51	1.19	3.54	1.88	0.11	0.05	0.05	0.04		23.0	1.0
DDH-177	7.57	0.65	2.08	2.69	1.96	0.13	0.04	0.03	0.01		23.0	1.0
EPIDOTE												
MF-0801	3.22	2.06	0.90	0.01	2.03	0.01		0.02			12.5	0.5
MF-1306	3.10	2.16	0.99	0.01	1.98	0.01	0.01	0.02	0.01		12.5	0.5
MF-2011	3.60	2.20	0.96	0.01	2.05	0.01	0.01	0.01	0.02		12.5	0.5
MF-2204	3.12	2.22	0.76	0.01	2.13	0.01		0.02			12.5	0.5
MF-2603	3.10	2.21	0.90		2.06	0.01		0.01			12.5	0.5
MF-2634	3.22	2.02	0.99	0.01	2.01			0.01			12.5	0.5
MF-2802	3.01	2.24	0.98	0.01	2.01	2.10	0.01	0.01	0.01		12.5	0.5
DDH-177	3.16	2.05	1.03	0.03	2.02			0.01			12.5	0.5
SALITE												
MF-0801	1.96	0.05	0.27	0.80	0.88	0.03		0.02	0.06		6.0	
MF-2204	1.95	0.05	0.24	0.80	0.96	0.03		0.02	0.03		6.0	
AUGITE												
MF-1708	1.98	0.05	0.29	0.76	0.86	0.04		0.01	0.01		6.0	1.0
HORNBLENDE												
MF-1708	6.20	2.10	1.24	3.54	1.77	0.60	0.21	0.03	0.23		23.0	1.0
MF-3005	6.45	1.96	1.77	2.79	1.90	0.38	0.21	0.02	0.18		23.0	1.0
PLAGIOCLASE												
MF-0804	2.59	1.42			0.41	0.57	0.01				8.0	
MF-1306	2.58	1.42			0.42	0.56	0.02				8.0	
MF-1504	2.56	1.44			0.44	0.55	0.01				8.0	
MF-1708	2.60	1.40			0.40	0.59	0.01				8.0	
MF-2011	2.60	1.40			0.40	0.59	0.01				8.0	
MF-2206	2.64	1.36			0.36	0.63	0.02				8.0	
MF-2603	2.64	1.36			0.36	0.62	0.02				8.0	

TABLE 4—(*Continued*)

	SI	AL	FE	MG	CA	NA	K	MN	TI	RA	O	H2O
MF-2802	2.66	1.34			0.34	0.64	0.02				8.0	
MF-3005	2.59	1.41			0.41	0.58	0.01				8.0	
DDH-812	2.63	1.37			0.37	9.61	0.01				8.0	
ON-3005	2.64	1.36			0.37	0.61	0.02				8.0	
VL-2002	2.68	1.32			0.32	0.66	0.02				8.0	
K-FELDSPAR												
MF-0804	2.99	1.01			0.01	0.12	0.87				8.0	
MF-1306	2.99	1.01			0.01	0.12	0.88				8.0	
MF-1708	2.99	1.01			0.01	0.14	0.85				8.0	
MF-2011	2.99	1.01			0.01	0.12	0.87				8.0	
MF-2206	2.99	1.01			0.01	0.13	0.86				8.0	
MF-2802	3.00	1.00			0.01	0.17	0.83				8.0	
MF-3005	3.00	1.00				0.12	0.88				8.0	
DDH-812	3.00	1.00			0.01	0.12	0.88				8.0	
ON-3005	2.99	1.01			0.01	0.12	0.87				8.0	
VL-2002	3.00	1.00				0.10	0.90				8.0	

procedure. The mass concentration, X_i, of the i^{th} element in a rock is determined by the relationship between the mass abundances of the n mineral phases, m_j, and the concentrations of the i^{th} element in the j^{th} mineral, $C_{i,j}$.

$$X_i = \sum_{j=1}^{n} m_j C_{i,j}. \tag{5}$$

A set of such equations can be written to represent the k rock-forming elements where $n \leq k$ is a required condition. The set of equations has the form:

$$\begin{aligned} m_1C_{11} + m_2C_{12} \ldots + m_jC_{1j} &= X_1 \\ m_2C_{21} + m_2C_{22} \ldots + m_jC_{1j} &= X_2 \\ \vdots \qquad\qquad\qquad\quad & \vdots \\ m_1C_{k1} + m_2C_{k2} \ldots + m_jC_{kj} &= X_k. \end{aligned} \tag{6}$$

In matrix notation, equation (6) becomes

$$mC = X \tag{7}$$

where C contains the chemical composition of the mineral phases, X the chemical composition of the rocks, and m the mineralogical composition of the sample. If the number of minerals is equal to the number of elements analyzed, i.e., if $n = k$, there will usually be a unique solution to (7). Hydrothermally altered rocks are generally disequilibrium assemblages; thus, the number of phases is not constrained to be less than or equal to the number of components. However, the number of major phases is commonly observed to be less than the components, and equation (7) is overdetermined. The solution to (7) is obtained by a least squares approximation in which the sum of the square of the difference between actual whole-rock chemical data and the value of X_i computed from (7) are minimized. Additional constraints are imposed whereby $\Sigma m_i = 1.0$, negative values of m_j are not allowed, and the solution is allowed, and the solution is weighted according to the estimated absolute error in the analytical data. Practical use of this method requires the selection of a representative mineralogy in terms of major minerals in order to obtain the best mineral fit from the computations.

Distribution of Major Mineral Constituents in the Altered Rocks

The thermal anomaly accompanying the emplacement of the Mayflower and Ontario stocks was largely dissipated by movements of fluids along open continuous fractures present in both igneous and adjacent rocks, as discussed previously. Observations in the fractured igneous rocks of the Mayflower mine reveal that permeable fractures are commonly filled with product minerals and enveloped by discrete halos of alteration phases (1–2 cm wide). As a result, large volumes of the stocks appear to have survived as relatively unaltered blocks of rock bounded by flow fractures. Diffusion channels cut

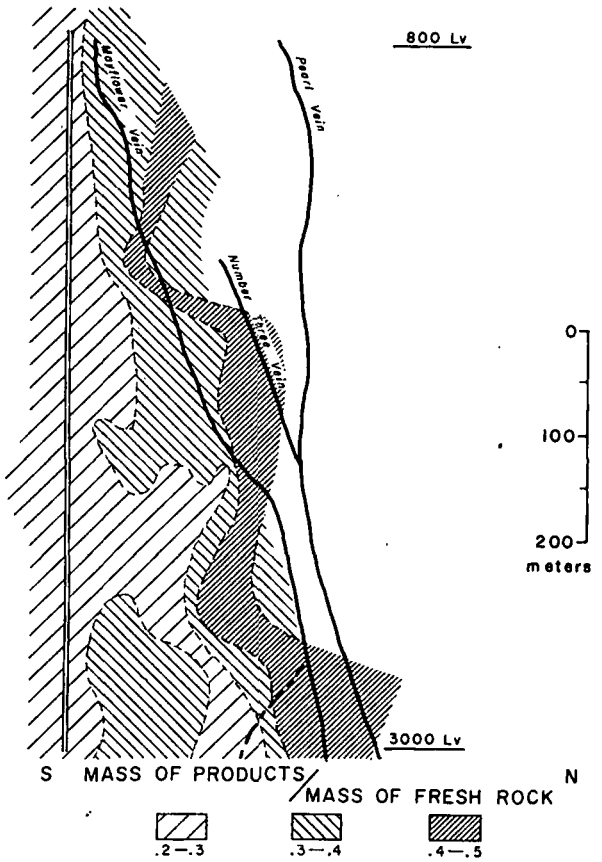

FIG. 16. Distribution of mass of alteration products in relation to mass of unaltered rocks in a portion of the Mayflower stock.

across these blocks as evidenced by tortuous alteration paths on the order of millimeters in width.

From this general picture, one is led to expect a major control of the flow fractures on the distribution of reactant and product minerals composing the altered Mayflower and Ontario stocks. The best evidence of this control comes from the overall mass distribution, as determined by regression, of the major minerals of the stock over a north-south cross section of the mine (Fig. 16), showing that the ratio of altered to unaltered assemblages increases toward the main vein system. Control on the distribution of individual minerals is evident for andesine, K-feldspar, kaolinite, and quartz (Figs. 17 to 20), the last three increasing in abundance toward the major veins. Andesine, the quantitatively most important reactant mineral, was more thoroughly destroyed in the vicinity of the major veins than in any other zone sampled. Biotite, chlorite, pyrite, anhydrite, and calcite distributions (Figs. 21 to 25), on the other hand, do not seem to depend on the main veins, although below the 2,600-ft level a lateral zoning is apparent, with biotite and chlorite increasing in abundance away from the Mayflower vein.

The distribution of the major minerals also disclosed a vertical zoning with calcite and quartz being more abundant above the 2,400-ft level of the mine and pyrite, anhydrite, K-feldspar, kaolinite, biotite, and chlorite more abundant below. The change in the relative abundance of anhydrite and calcite with depth may reflect an increase in the $a_{CO_3^{2-}}/a_{SO_4^{2-}}$ ratio in the solutions which favored the precipitation of calcite as the CO_2 pressure increased. This chemical change may have been a consequence of solutions flowing from quite distinct sedimentary sequences, below and above the horizons that mark the upward transition from more clastic to more calcareous formations. This transition occurs at a depth corresponding approximately to the 2,400-ft level (Fig. 26). As a result, the inflow of solutions that might have been in equilibrium with carbonate rocks was largely favored at depths above that level, and precipitation of calcite occurred as the relatively high CO_3 solutions moved into the pluton. Likewise, SO_4^{2-}-rich solutions, possibly in equilibrium with the basement rocks, might have entered the system from below to cause the observed vertical zoning, with

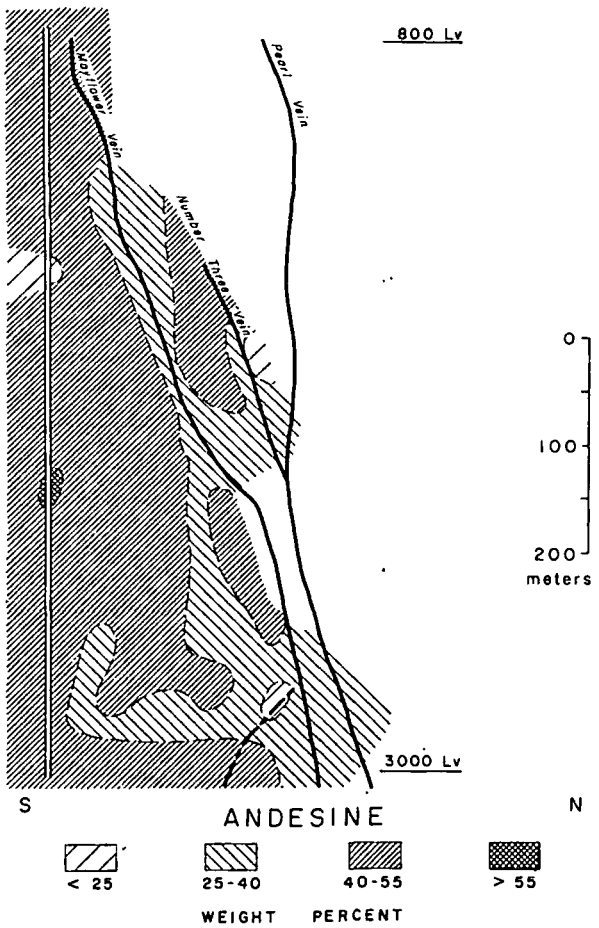

FIG. 17. Distribution of andesine in the Mayflower stock.

sulfate largely consumed at greater depths as anhydrite precipitated. Equilibrium relations show that at lower reaction temperatures, for a given CO_2 pressure and SO_4^{2-} constant, calcite has its stability field expanded over that of anhydrite, suggesting that temperature may have also contributed to larger ratios of calcite to anhydrite at shallower depths. Pyrite was found to be more abundant below the 2,600-ft level at some distances south of the Mayflower vein.

A collective picture of the variational trends of the major minerals is shown along north-south traverses on the 2,800-ft level across the Mayflower-Ontario contact (Fig. 27); it relates the abundances of reactant and product phases with distance from the main vein structure.

Gains and Losses of Components

The comparison between altered and unaltered compositions of rock samples affords a quantitative estimate of the irreversible reactions that took place between hydrothermal solutions and rocks. The extent of these reactions in the Mayflower mine is indicated by the variation of ratios between the masses of product and reactant minerals, which shows that the greatest change in mineralogy occurred in the regions closer to the Mayflower vein (Fig. 16). From data on chemical and mineralogical compositions of altered and unaltered rocks, the overall mass transfer in the stocks could be appraised in terms of gains and losses of both minerals and components. Bulk densities were determined on all samples in order to compute gains and losses. Lack of visible microscopic or megascopic deformational features in the altered zones of the Mayflower and Ontario stocks is supporting evidence that no significant volume change took place during alteration so that densimetric percentages could be used to represent rock compositions without introducing errors. Bulk density variations resulting from the hydrothermal processes were thus caused by the addition or removal of mass from the rocks.

Mineral abundances and gains and losses of minerals and major elemental components in the Mayflower stock, determined by regression, are sum-

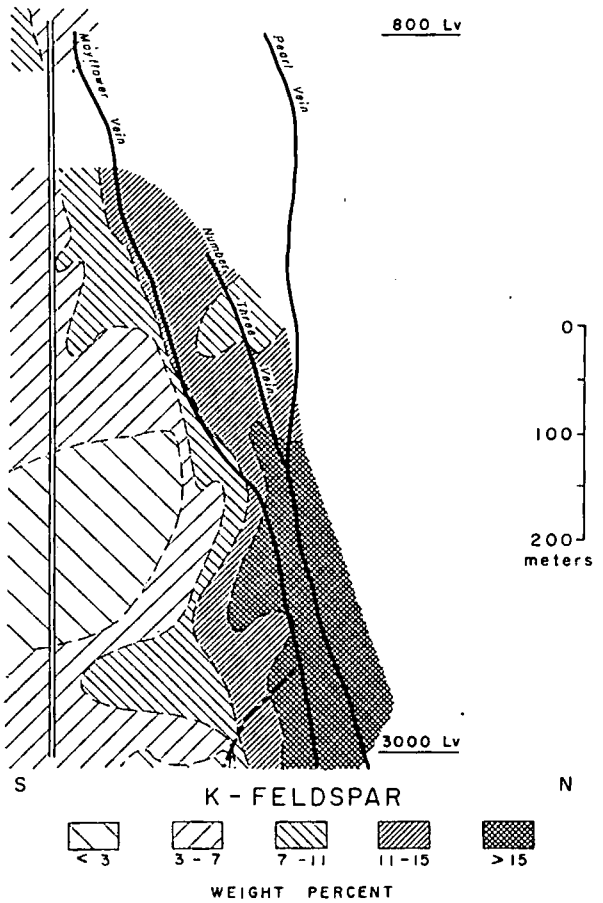

FIG. 18. Distribution of K-feldspar in the Mayflower stock.

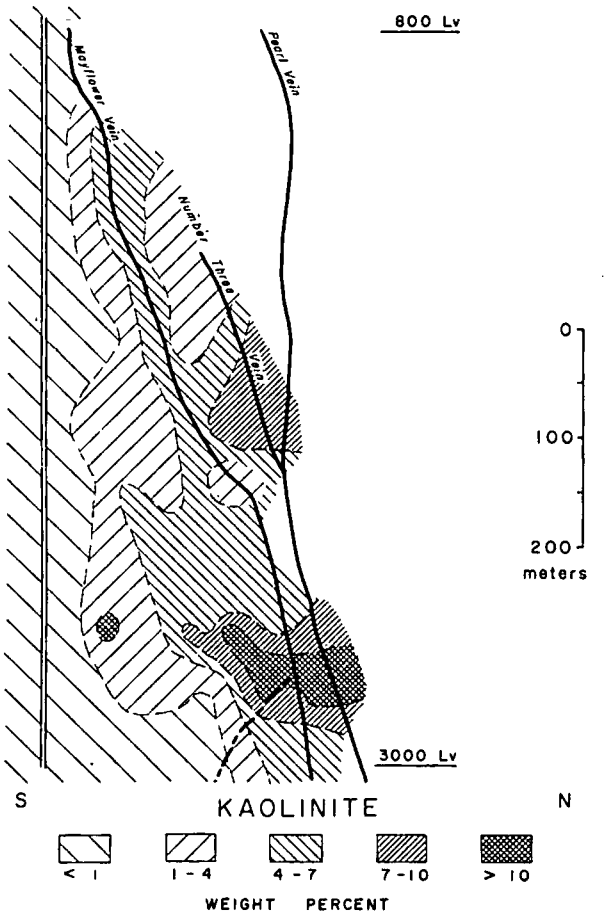

FIG. 19. Distribution of kaolinite in the Mayflower stock.

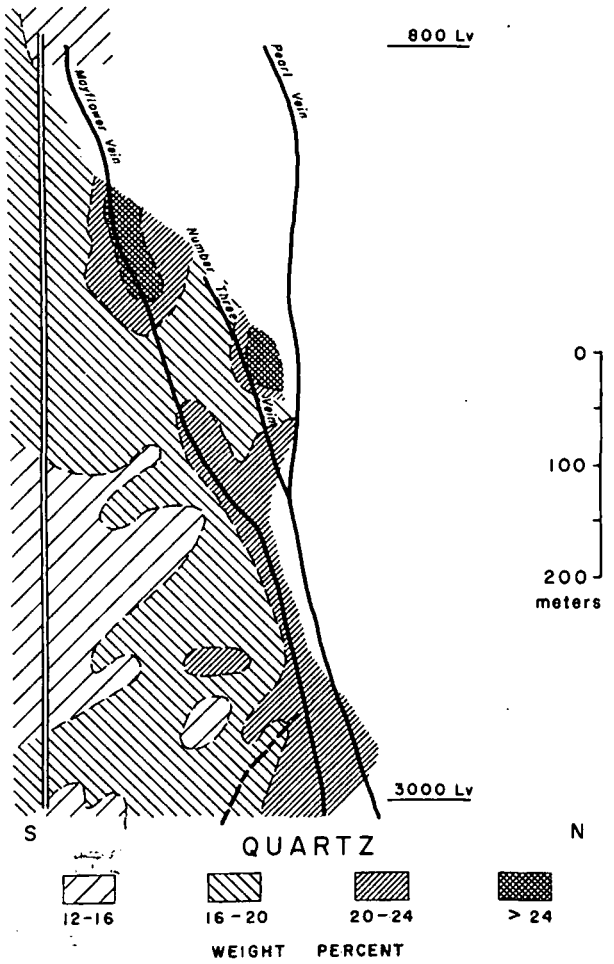

FIG. 20. Distribution of quartz in the Mayflower stock.

marized in Table 5. Gains and losses of minerals are reported either as the range of variation for all sampled traverses or as the average mass balance for distinct altered blocks in the north-south cross section (Fig. 28). Gains and losses of elemental components are shown as average values in either case. The division of the vertical section into blocks of alteration was based on the distribution of relative amounts of major minerals and was done in order to compare systematically the observed mass transfer with that predicted by theoretical computations. Average mineral masses are also presented, and their variation from block to block reiterates the earlier recognition of a broad zone of alteration in the mine.

From the mineralogical gain and loss tabulation, it can be seen that greater masses of andesine were destroyed than any other reactant mineral, followed by igneous biotite and hornblende. The other reactant phases were either consumed or reequilibrated with the hydrothermal solutions but were subsequently added to the rocks as alteration products. Anhydrite, calcite, pyrite, kaolinite, chlorite, and albite occur exclusively as alteration products. The original mass of hornblende (0.08 g/cm^3) was assumed to be totally consumed during alteration, despite its preservation in some rock pulps (generally in amounts less than 1%, a condition that excludes it from the mineral abundance calculations). Similarly, the igneous biotite (0.32 g/cm^3) was assumed to be completely destroyed or reequilibrated to the composition of the present hydrothermal biotite. Hence, the values of hornblende and igneous biotite appear as losses equivalent to their respective original amounts, regardless of the alteration zone to be considered.

The mass balance for the sampled rocks indicates an overall loss of Si, Al, Na, and Ca and an overall gain of Fe (total), Mg, K, S, C, and Ti. Large quantities of sulfide and sulfate were added to the altered rocks from the hydrothermal solutions by reaction with indigenous iron and calcium in the wall rocks. The latter were almost exclusively deposited

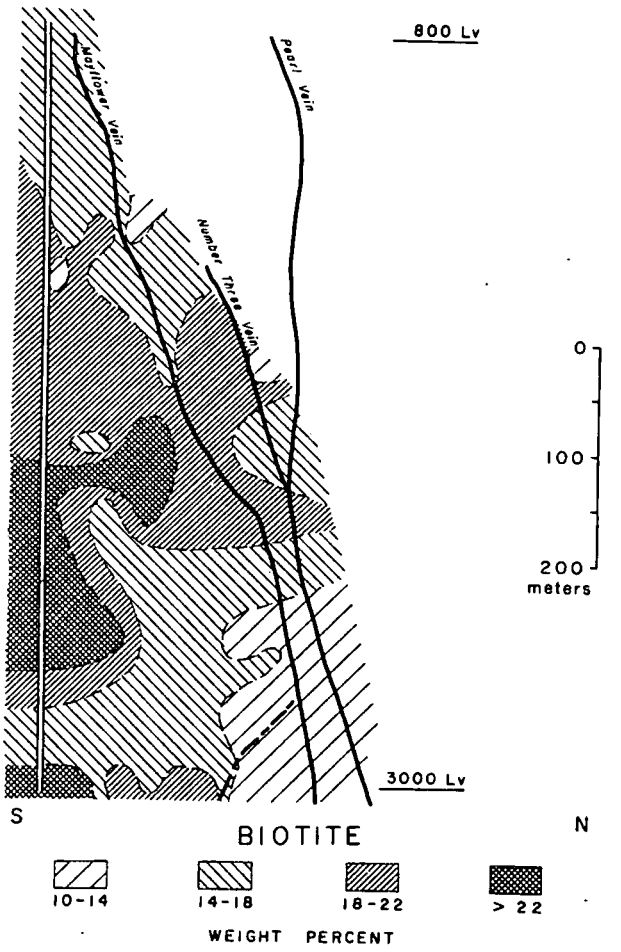

FIG. 21. Distribution of biotite in the Mayflower stock.

in the ore zone as sulfides. A portion of the total sulfur was in the form of sulfate which was incorporated into the altered rocks mainly as anhydrite. Considerable addition of CO_3^{2-} was also evident, as the widespread occurrence of calcite indicates.

Comparison of Predicted with Observed Mineral Abundances

Circulation of fluids along pathlines between different chemical environments apparently resulted in the mineral abundances and elemental gains and losses that were measured. As a fluid packet circulates from one chemical environment into another, mass transfer occurs between the fluid and rock along its flow path. On the basis of the conditions predicted by the heat transfer calculations and an estimation of initial solution concentrations, the alteration process can be simulated by theoretical methods. Helgeson et al. (1970) describe methods which simulate the overall mass transfer resulting from irreversible reactions between a fixed quantity of aqueous solution and initial reactant mineral assemblages. Equilibrium

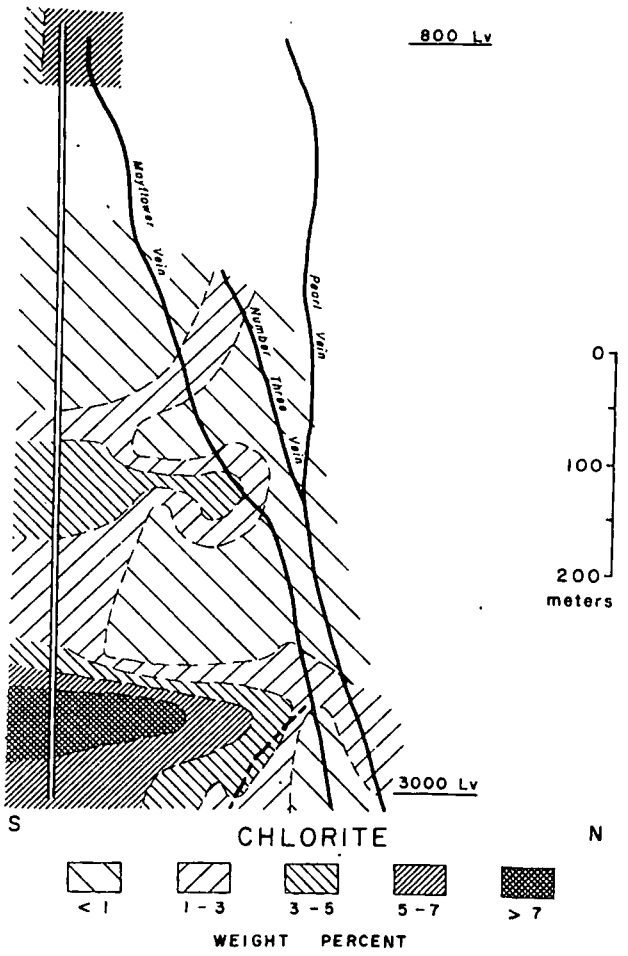

FIG. 22. Distribution of chlorite in the Mayflower stock.

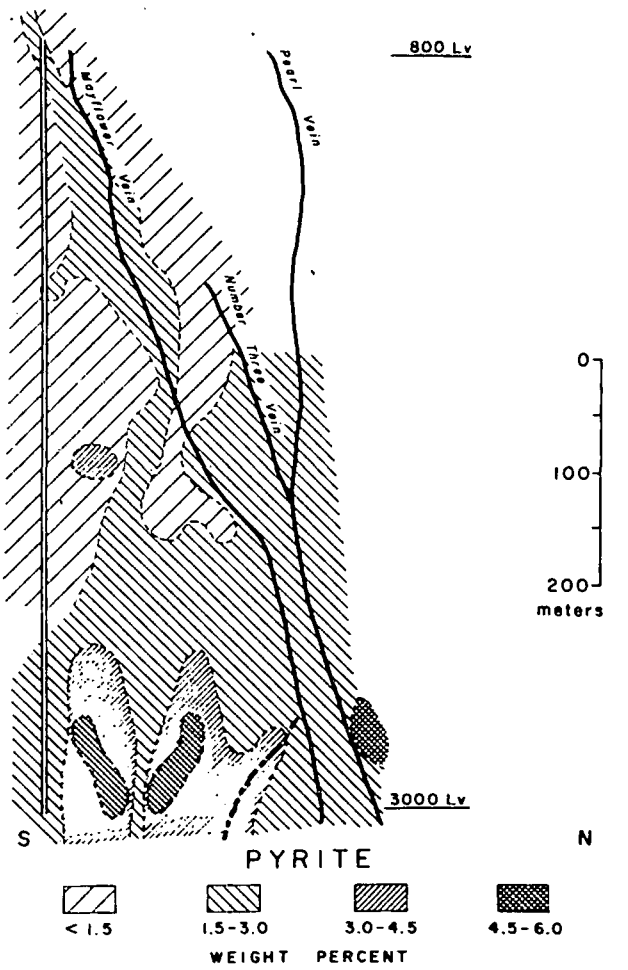

FIG. 23. Distribution of pyrite in the Mayflower stock.

conditions are defined by a set of differential equations describing the laws of mass action and mass and charge balances at a fixed temperature and pressure; and the overall irreversible reaction is approximated by the derivatives of these variables with respect to the reaction progress.

The thermal regime of the igneous wall rocks and fluids that prevailed over discrete periods of time during the cooling history of the Mayflower stock was used to define conditions for which the fluid-rock reactions were simulated. The heat flow computations predict that during the major portion of the cooling process temperatures were in the 150° to 400°C range, but the thermodynamic data for the mass transfer computations was only available for 25° to 300°C and 1 bar; therefore, fluid-rock reactions could be simulated only at a sequence of discrete temperatures between 300° and 150°C. Modeling of the cooling history of the Mayflower stock has shown that its top regions remained at temperatures significantly above 300°C only for the initial 1.5×10^4

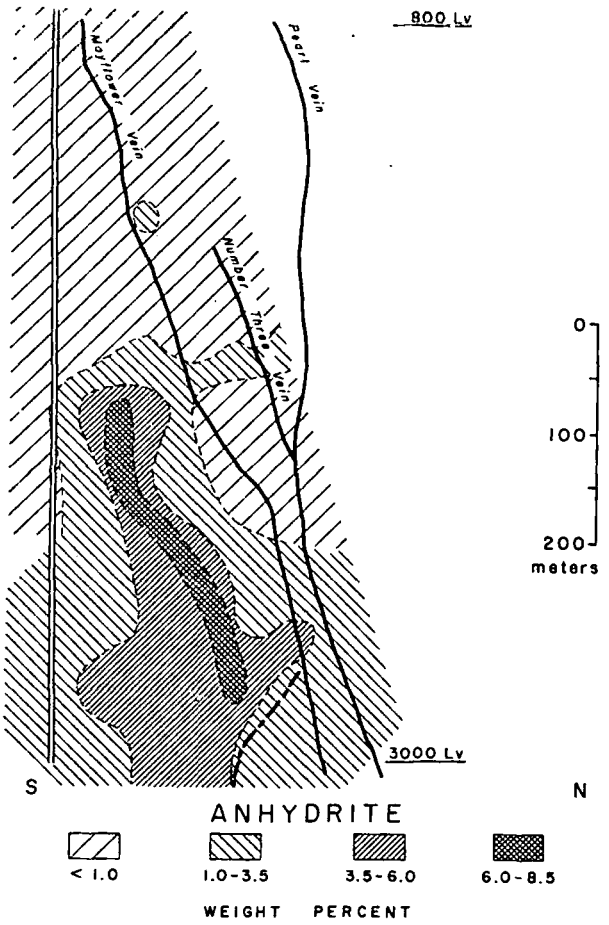

FIG. 24. Distribution of anhydrite in the Mayflower stock.

years subsequent to the vent that fractured and enabled fluid circulation through the upper 1.5 km of the stock, so that the 300°C restriction probably does not affect the results significantly. The unaltered equivalents of Mayflower rocks were taken as initial reactant assemblages, and initial solution compositions were estimated on the basis of fluid inclusion studies, which indicate high salinity fluids (34–44 equiv. wt % NaCl), suggest relatively low Na/K ratios in the fluid and filling temperatures of 350° ± 50°C for the earliest stages of vein formation in the Mayflower stock (Nash, 1973). Additional constraints in the solution compositions relied upon equilibrium relationships among the alteration assemblages at a given temperature (Villas, 1975).

Fluid circulation caused by the Mayflower stock clearly caused mixing of H_2O-rich magmatic fluids with aqueous solutions entering from the surrounding host rocks. The nature of fluid pathlines not only indicates the inevitable mixing of fluids from various sources, but also the drastic changes in pressure and temperature along the pathlines that affect the thermodynamic properties of the solvent (Norton and Knight, 1977). Dilution of high salinity fluids in the Mayflower stock is also evidenced by analysis of fluids included in quartz and sphalerite crystals, present in the major veins, which revealed salinities ranging from 0.3 to 11 weight percent NaCl equivalent (with average around 5 wt %) and homogenization temperatures between 220° and 300°C (Nash, 1973). Provisions for dilution were incorporated into the mass transfer calculations by assuming progressively more dilute starting solutions at the lower temperatures. Solutions initially reacted with the Mayflower rocks at 300°C had true ionic strengths around 5.0, comparable to the lower limit for the salinities characteristic of the early vein minerals (~30 wt % NaCl equivalent), whereas the more dilute solutions, below 200°C, had true ionic strengths of 0.3. This dilution process is consistent with the large influx of fluids from the host rocks which could dilute initial high-salinity fluids by at least a factor of 10, if we presume the host rock fluids are ~0.1 m.

General characteristics of the starting solutions for the mass transfer reactions used to simulate the

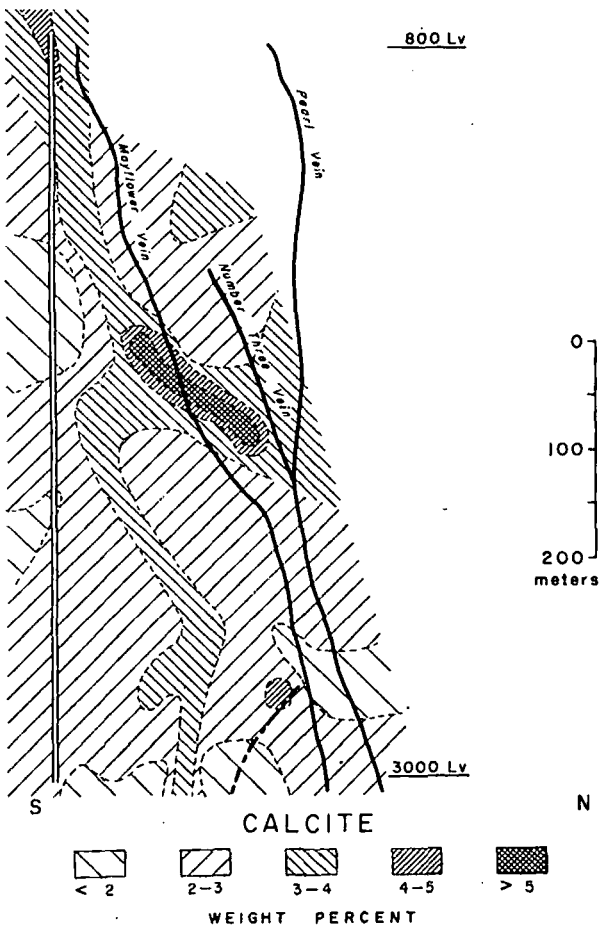

FIG. 25. Distribution of calcite in the Mayflower stock.

alteration of the Mayflower stock are presented in Table 6. These solutions were selected on the basis of observed mineral assemblages, gains and losses of elemental components, and inferred compositions of circulating fluids. Additional initial conditions included: (1) oxygen fugacity fixed at a given temperature for the pyrite-magnetite and pyrite-hematite pairs which were commonly observed in the alteration assemblages; (2) starting solutions in equilibrium with quartz and pyrite; (3) CO_2 pressure fixed at an upper limit of 10 bars; (4) $CO_2(g)$ as a reactant only at temperatures below 200°C; and (5) reaction rates of reactant solid phases proportional to their original mole fractions in the unaltered rocks.

Results of Mass Transfer Calculations

The irreversible reaction paths between solutions and the unaltered equivalents of the Mayflower rocks are represented in activity-activity diagrams which depict the stability fields of minerals and the compositions of the solutions that coexist with these minerals. The composition of the starting solution at 300°C is in equilibrium with both pyrite and quartz and projects onto the microcline stability field (Fig. 29). Incremental masses of reactants dissolved in the solution caused its composition to shift initially toward

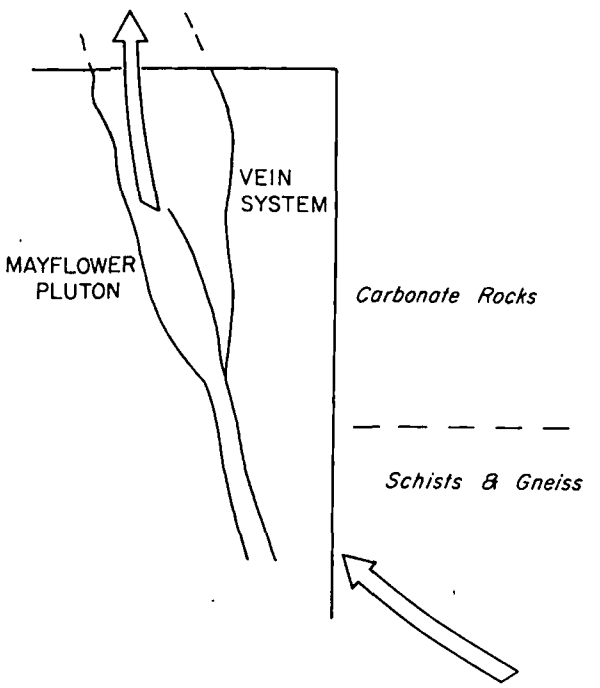

FIG. 26. Schematic north-south cross section of the vein system in the Mayflower stock, showing major types of host rocks and direction of fluid flow. The upward transition from clastic to calcareous rocks occurs at a depth corresponding approximately to the 2,400-ft level of the mine.

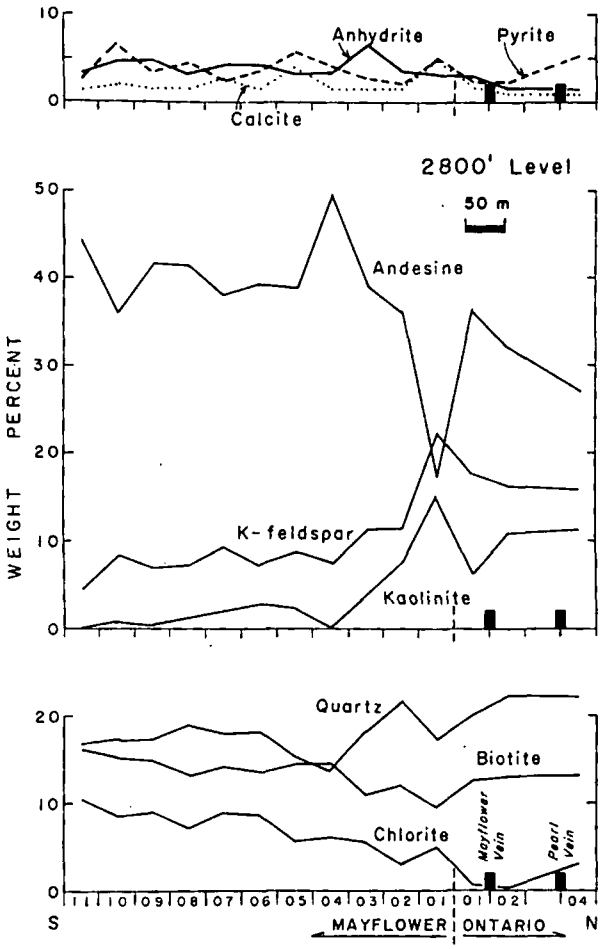

FIG. 27. Lateral variation of the abundance of the major mineral constituents of the Mayflower and Ontario stocks with respect to the vein system on the 2,800-ft level.

higher $a_{Mg^{2+}}/a^2_{H+}$ ratios at an essentially constant $a_{Fe^{2+}}/a^2_{H+}$ ratio, since the solution was enriched in Mg as a result of dissolution of igneous biotite, whereas the Fe derived from the destruction of biotite and magnetite was consumed by the production of pyrite. This portion of the reaction path was followed by precipitation of anhydrite, then by muscovite, Figure 30. However, near the Mg-montmorillonite-phlogopite boundary, muscovite ceased being produced. The solution next equilibrated with Mg-montmorillonite but then undersaturated with respect to quartz and, at the same time, started precipitating phlogopite. Further dissolution of igneous biotite and simultaneous precipitation of phlogopite and Mg-montmorillonite maintained the $a_{Mg^{2+}}/a^2_{H+}$ ratio constant, shifting the solution composition toward equilibrium with biotite. In the process, Mg-montmorillonite, phlogopite, and pyrite became undersaturated, favoring the precipitation of Mayflower biotite and Ca-montmorillonite. By the time overall

TABLE 5. Mineral Abundances and Gains and Losses of Minerals and Elemental Components in the Mayflower Stock

Minerals	Mineral abundances					Gains and losses					Range of variation for all traverses	
	Grams of minerals/cm³ of rock										Gains	Losses
	Block 1	Block 2	Block 3	Block 4	Block 5	Block 1	Block 2	Block 3	Block 4	Block 5		
Andesine	0.98	1.19	1.25	1.08	1.24	−0.92	−0.72	−0.70	−0.86	−0.60		0.17–1.04
K-feldspar	0.41	0.16	0.18	0.33	0.17	0.27	0.03	0.00	0.18	0.03	0.47 to	0.13
Quartz	0.54	0.47	0.43	0.58	0.44	0.26	0.20	0.21	0.28	0.21	0.00–0.46	
MF-biotite	0.35	0.47	0.49	0.52	0.51	0.35	0.47	0.49	0.52	0.51	0.26–0.70	
Pyrite	0.08	0.11	0.05	0.05	0.04	0.08	0.11	0.05	0.05	0.04	0.06–0.18	
Calcite	0.05	0.04	0.05	0.09	0.06	0.05	0.04	0.05	0.09	0.06	0.01–0.60	
Anhydrite	0.08	0.10	0.08	0.02	0.06	0.08	0.10	0.08	0.02	0.06	0.00–0.24	
Chlorite	0.05	0.18	0.05	0.03	0.05	0.05	0.18	0.05	0.03	0.05	0.00–0.29	
Kaolinite	0.18	0.01	0.11	0.14	0.05	0.18	0.01	0.11	0.14	0.05	0.00–0.41	
Magnetite	—	—	—	0.01	0.02	−0.03	−0.03	−0.03	−0.02	−0.01		0.00–0.03
Hornblende*	—	—	—	—	—	−0.08	−0.08	−0.08	−0.08	−0.08		0.08
Biotite*	—	—	—	—	—	−0.32	−0.32	−0.32	−0.32	−0.32		0.32
Albite	—	—	—	—	—	—	—	—	—	—	0.00–0.43	
Grain density	2.72	2.73	2.69	2.85	2.64							

Elements	Gains and losses					Average for all traverses	
	Grams of components/cm³ of rock					Gains	Losses
Si	0.010	−0.040	−0.026	0.000	−0.032		0.009
Al	−0.043	−0.061	−0.044	−0.052	−0.050		0.049
Fe(total)	−0.009	0.028	0.003	0.002	0.004	0.006	
Mg	0.011	0.049	0.032	0.021	0.028	0.026	
Ca	−0.024	0.002	0.010	−0.024	0.023		0.011
Na	−0.035	−0.031	−0.031	−0.041	−0.034		0.032
K	0.032	0.014	0.015	0.032	0.017	0.021	
S	0.043	0.068	0.027	0.034	0.024	0.038	
C	0.006	0.005	0.007	0.011	0.011	0.007	
SO_3	0.048	0.062	0.051	0.011	0.031	0.037	
Ti	0.009	0.013	0.013	0.012	0.013	0.010	

* Hornblende was assumed to be totally destroyed for purposes of computing mineral abundances of major minerals. Igneous biotite was assumed to be destroyed or reequilibrated to hydrothermal biotite (MF-biotite).

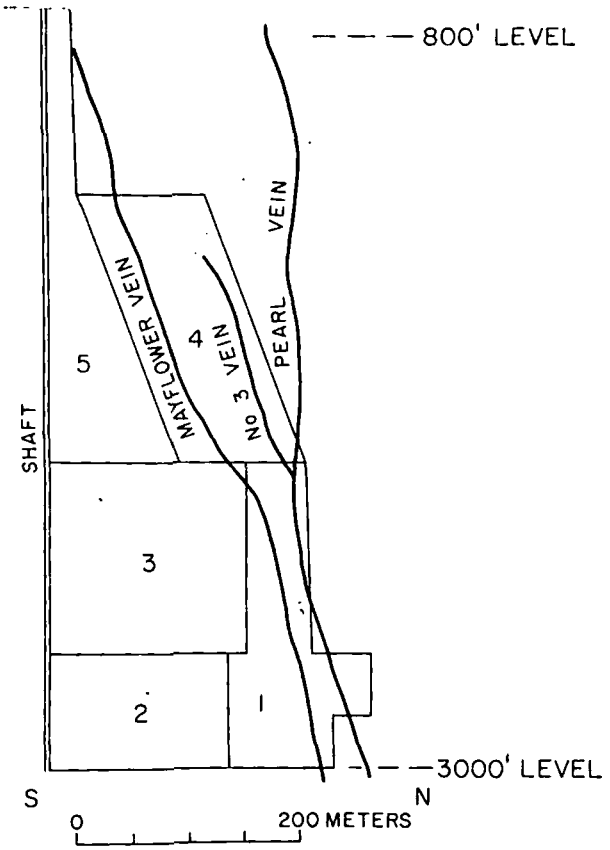

FIG. 28. Blocks of alteration over a north-south 670 m cross section in the Mayflower stock that were defined on the basis of abundances of major alteration products (see Table 4).

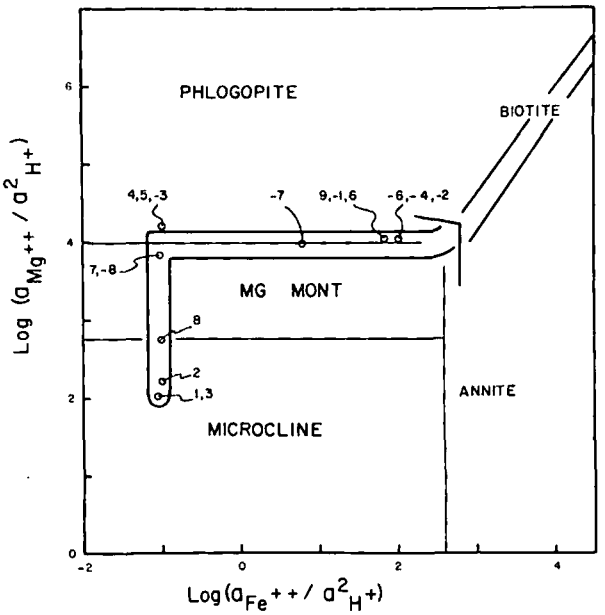

FIG. 29. Activity diagram for the system MgO-FeO-K_2O-Al_2O_3-SiO_2-HCl-H_2O at 300°C and 1 bar. Activity of solid phases and H_2O are equal to one; equilibrium reactions were balanced on aluminum. Log $a_{H_4SiO_4} = -1.94$, quartz saturation and log $(a_{K^+}/a_{H^+}) = 4.0$. Reaction path at 300°C (refer to Fig. 30) on activity diagram shows the shift in solution composition as the reaction progressed. The tail of the arrow represents the composition of the starting solution, whereas the small circles mark the positions at which a product phase either started (positive numbers) or ceased (negative numbers) precipitating out of the solution. Mg-mont = magnesium-montmorillonite. Biotite represents stability field for biotite found in the Mayflower altered igneous rocks.

equilibrium was reached, 130 g of reactant phases were destroyed, and 150 g of product phases were formed per kilogram of water, with a net change in pH from 4.5 to 4.7, Table 7.

The starting solution at 200°C (Fig. 31) was initially in equilibrium with quartz, pyrite, and Ca-montmorillonite. As reactants dissolved, the solution composition shifted parallel to the Ca-montmorillonite–Na-montmorillonite boundary. The solution then equilibrated with calcite, whose saturation surface for a CO_2 fugacity of 9.5 bars was reached at log $(a_{Ca^{2+}}/a^2_{H^+}) = 7.47$ and after 0.57 g of andesine

TABLE 6. Initial Solution Compositions for Path Reactions at Different Temperatures (molality)

Species	300°C	250°C	200°C	150°C
Al^{3+}	1.0×10^{-9}	1.0×10^{-9}	1.0×10^{-9}	1.0×10^{-9}
K^+	2.5	2.5	2.5×10^{-2}	2.5×10^{-2}
Na^+	3.2	3.2	3.2×10^{-1}	3.2×10^{-1}
Ca^{2+}	2.2×10^{-3}	1.3×10^{-3}	1.3×10^{-3}	1.3×10^{-3}
Mg^{2+}	3.7×10^{-6}	3.7×10^{-6}	3.7×10^{-5}	3.7×10^{-5}
Fe^{2+}	7.4×10^{-10}	2.6×10^{-10}	1.0×10^{-9}	1.0×10^{-7}
Cu^+	1.0×10^{-3}	1.0×10^{-3}	1.0×10^{-7}	1.0×10^{-6}
H_4SiO_4	1.2×10^{-2}	7.8×10^{-3}	4.5×10^{-3}	2.1×10^{-3}
S^{2-}	8.0×10^{-2}	2.4×10^{-2}	1.0×10^{-3}	1.0×10^{-6}
SO_4^{2-}	9.5×10^{-3}	5.6×10^{-2}	2.8×10^{-2}	2.5×10^{-2}
CO_3^{2-}	1.0×10^{-3}	1.0×10^{-3}	7.8×10^{-2}	7.7×10^{-2}
Cl^-	4.4	4.4	4.7×10^{-1}	3.5×10^{-1}
Initial pH	4.50	4.40	4.50	4.50
Final pH	4.68	4.82	6.25	6.56
True ionic strength	5.32	5.36	0.54	0.32

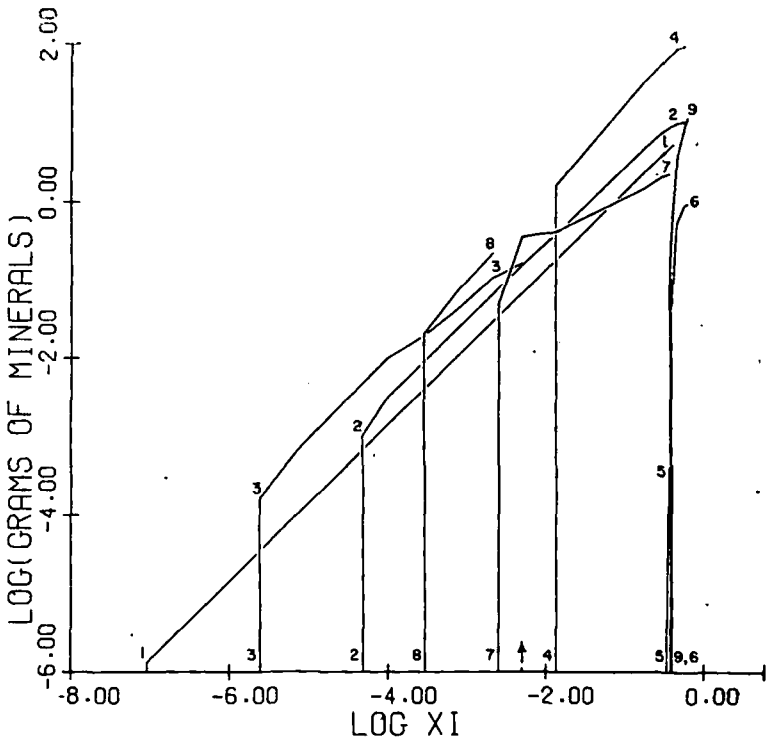

FIG. 30. Masses of alteration minerals produced, per 1,000 g of solution, as a function of reaction progress during reaction of unaltered Mayflower igneous assemblages and solutions at 300°C. Arrow marks position with respect to reaction progress when phlogopite equilibrated with the solution. Indices refer to curves that represent precipitation of alteration minerals in systems where 1 = pyrite, 2 = anhydrite, 3 = quartz, 4 = microcline, 5 = phlogopite, 6 = Ca-montmorillonite, 7 = Mg-montmorillonite, 8 = muscovite, and 9 = biotite. Calculations based on thermodynamic data from Helgeson (1969).

per kilogram of water had been destroyed. Calcite equilibration constrained the solution composition to shift along the calcite saturation surface. Increases of H in log a_{Na^+}/a_{H^+} relative to log $a_{Ca^{2+}}/a^2_{H^+}$ changed the solution composition toward the Ca-montmorillonite–Na-montmorillonite low albite phase equilibrium point. Phlogopite and alteration muscovite became stable, but Ca-montmorillonite ceased precipitating. The solution then equilibrated with Na-montmorillonite and low albite, at which time only 22 g of product phases had been formed. Thereafter, as the reaction progressed, significantly larger mass transfer occurred and, when overall equilibrium was attained, 166 g of products had been precipitated as opposed to 163 g of reactants destroyed per kilogram of water (Fig. 32 and Table 7).

The saturation surface of anhydrite shifted as calcite precipitated, from a position at log $(a_{Ca^{2+}}/a^2_{H^+}) = 8.2$ when the solution first saturated with calcite to a position at log $(a_{Ca^{2+}}/a^2_{H^+}) = 9.8$ by the time

TABLE 7. Irreversible Mass Transfer at 300°C and 200°C

	Reactants 300°C		Reactants 200°C	
	Log mass destroyed	Log mass produced	Log mass destroyed	Log mass produced
Magnetite	0.2	—	−2.0	0.8
Quartz	1.5	−0.8	−4.7	0.7
Microcline	−0.8	2.1	1.0	—
Annite	1.0	—	1.1	—
Phlogopite	0.9	−3.4	−0.8	−0.9
Mayflower plagioclase	1.9	−7.6	2.1	—
Carbon dioxide			1.0	−8.4
Initial pH	4.5		4.5	
Final pH	4.7		6.3	

overall equilibrium was attained. At 200°C production of calcite prevented the solution from saturating with respect to anhydrite. This may partly explain the occurrence of larger masses of calcite than anhydrite in the shallower depths of the mine, as discussed earlier. The style of mass transfer between the aqueous phase and rock for reactions simulated at other temperatures (250° and 150°C) is similar to that documented for 300° and 200°C.

Comparison of Measured and Predicted Mineral Abundances

Predicted gains and losses of minerals were estimated from the amounts of minerals produced or destroyed on the basis of the mass transfer computations and from mass fluxes derived from analysis of fluid flow associated with the initial 1.8×10^5 years of cooling of the Mayflower stock. The mass flux estimates apply to the upper 1.5 km of the stock, whose temperatures remained at 350° to 300°C, 300° to 250°C, 250° to 200°C, and 200° to 150°C for periods of approximately 10^4, 6×10^4, 1.8×10^5, and 2.0×10^5 years, respectively. The last two periods were linearly extrapolated from the initial 1.8×10^5 years of cooling. Mass fluxes corresponding to these time intervals (Table 8) refer to the mass of fluids that flowed through a volume of rock with length measured vertically on the cross section of the stock.

Densimetric amounts of minerals (M_p, in grams of minerals per cm³ of rock) produced or destroyed in the computed irreversible reactions were calculated from

$$M_p = \frac{Wq\Delta t}{l} 10^{-3} \qquad (8)$$

where W is the computed amount of mineral produced or destroyed per kilogram of water, q is the total mass flux in g/cm²s, Δt is the time interval in seconds, and l, in cm, is the flow path length through a given volume of rock.

The predicted and observed gains and losses of minerals (Fig. 33 and Table 9) show a remarkable agreement for most minerals, considering the nature of the approximations made in the theoretical predictions and error in the observed data. The theory indicates much more microcline was added to the initial rock than was detected in the measurement. Conversely, the theory predicted quartz was removed from the rock, but in reality the quartz content increased. One possible explanation is the somewhat unusually large Na/K ratios in the initial solution. These ratios were estimated from the occurrence of halite and sylvite in the fluid inclusions (Nash, 1973) and may be too high since a decrease in potassium in the original solution would lead to the formation of

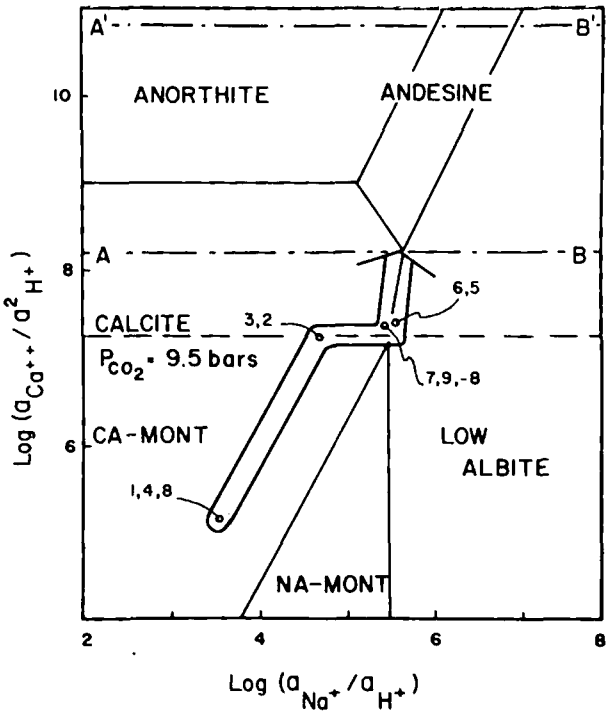

FIG. 31. Activity diagram for the system MgO-FeO-K_2O-Al_2O_3-SiO_2-HCl-H_2O at 200°C and 1 bar. Activity of solid phases and H_2O are equal to one; equilibrium reactions were balanced on aluminum. Log $a_{H_4SiO_4} = -2.35$, quartz saturation. Reaction path at 200°C (refer to Fig. 32) on activity diagram shows the shift in solution composition as reaction progressed. The tail of the arrow represents the composition of the starting solution, whereas the small circles mark the positions at which a product phase either started (positive numbers) or ceased (negative numbers) precipitating out of solution. A-B and A'-B' are the saturation surfaces for anhydrte at ξ values where calcite started precipitating and at the time the system attained overall equilibrium, respectively.

less microcline and, consequently, more quartz. Chlorite was approximated by clinochlore because thermodynamic data do not exist on chlorites with a composition similar to those found in the altered Mayflower igneous rocks, which may explain the fact that chlorite did not appear as a product phase in the computed irreversible reactions. Similarly, end members of the montmorillonite group were included as possible product phases in the irreversible reactions, due to a lack of thermodynamic data on intermediate members. This necessary approximation, together with the uncertainty in the end-member data, most likely stabilized the montmorillonites over other phases, causing large predicted amounts of these clays. As a result, these clays were equated to observed amounts of kaolinite.

The predicted mass abundances clearly indicate that many of the limitations imposed by the very simple coupling of the fluid flow and irreversible mass

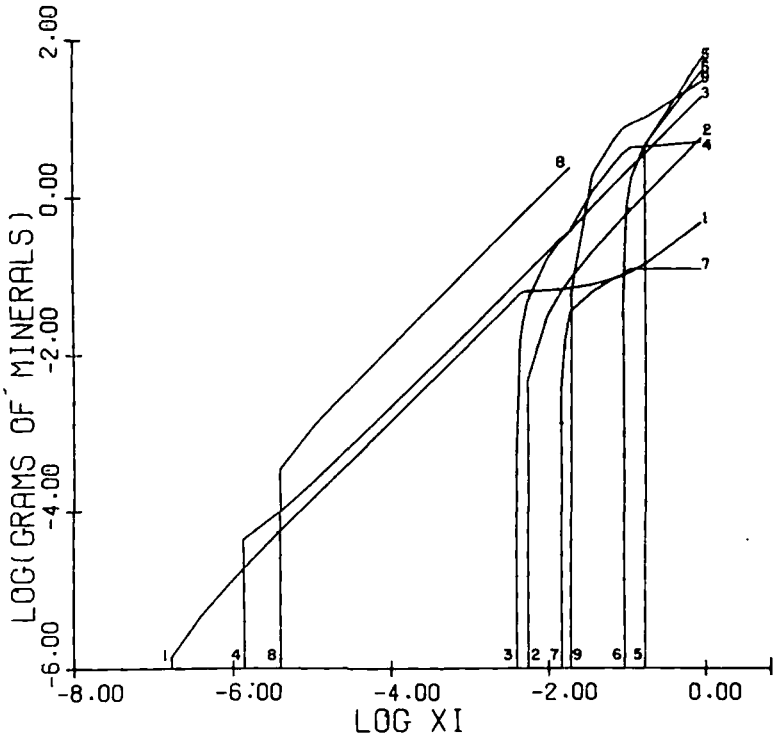

FIG. 32. Masses of alteration minerals produced, per 1,000 g of solution, as a function of reaction progress during reaction of unaltered Mayflower igneous rocks and solutions at 200°C. Indices refer to curves that represent precipitation of alteration minerals in open systems where 1 = pyrite, 2 = magnetite, 3 = calcite, 4 = quartz, 5 = low albite, 6 = Na-montmorillonite, 7 = phlogopite, 8 = Ca-montmorillonite, and 9 = muscovite. Calculations based on thermodynamic data from Helgeson (1969).

transfer theories must be accounted for in order to use transport theory to predict the mass abundance and distribution of phases in hydrothermal systems. But, for a first order approximation, the results are quite encouraging.

Conclusions

The igneous event that produced the Mayflower stock resulted in the development of abundant continuous fractures within the stock as it cooled below solidus temperatures. This fracturing generated permeabilities in the darcy range and allowed relatively large masses of fluids to circulate in and out of the stock. This convective transfer of heat cooled the entire stock to 0.3 of the initial thermal anomaly in 1.8×10^5 years, which is approximately 1.5 times faster than if the rock were impermeable and cooled by pure conduction. A large mass of hydrothermal fluid, 10^{13} kg per km of strike length, flowed through the upper 1.5-km portion of the stock during this same time period. These fluids circulated from a variety of rock environments, and along their pathlines they encountered variations in temperature and pressure. Irreversible mass transfer between these fluids and the Mayflower stock altered the stock to mineral assemblages that reflect the chemical composition of the rocks through which the fluids circulated, the pressure and temperature conditions along the flow paths, and initial composition of the fluids.

The heat and mass transport model of the Mayflower system provides a first order approximation

TABLE 8. Mass Fluxes that Prevailed in the Upper 1.5 Km of the Mayflower Stock during Cooling

	Time intervals (years)			
	10,000	60,000	180,000	200,000
Temperature range	350°–300°C	300°–250°C	250°–200°C	200°–150°C
Mass fluxes (g/cm^2 s)	1.6×10^{-7}	1.8×10^{-7}	4.0×10^{-8}	2.0×10^{-8}

of the temperature, pressure, and fluid fluxes that may have been realized in the natural system. These variables in turn define the conditions under which alteration and mineralization of the Mayflower stock occurred.

An analysis of the Mayflower hydrothermal system was based on quantitative data on the mineralogy and fluid inclusions combined with theoretical predictions of mass transfer and analysis of fluid flow in and around the Mayflower stock. The assumed solution compositions, prevalent pressure and temperature during the hydrothermal process, and the estimated amounts of fluids that circulated through the upper 1.5 km of the Mayflower stock as it cooled, predict the formation of mineral assemblages in masses similar to those found in the altered Mayflower igneous rocks. The mass transfer that resulted from irreversible reactions between the circulating fluids and the igneous rocks added relatively large amounts of S, C, K, Mg, and H_2O to the stock. The vertical zoning characterized by larger masses of calcite than anhydrite above the 2,400-ft level of the mine may reflect precipitation from fluids that circulated through different stratigraphic horizons and entered the stock at different depths. Fluids derived from the stratigraphically upper-carbonate host rocks were enriched in CO_3^{2-} content which favored the precipitation of calcite upon reaction with the andesine of the stock. Decrease in temperature and increase in CO_2 pressure further favored the precipitation of calcite over anhydrite in the shallower depths of the mine.

This analysis of the Mayflower hydrothermal system suggests that the original igneous minerals were altered by acid-sulfate solutions at moderate temperatures, <400°C, and pressures <1 kb. In order to account for the observed masses and compositions of alteration products, fluid fluxes on the order of 10^{-7} g/cm^{2}s^{-1} are required for at least 2×10^5 years. Although the hypothetical solution contained on the order of 50 ppm total copper, only small amounts of chalcopyrite were precipitated along the

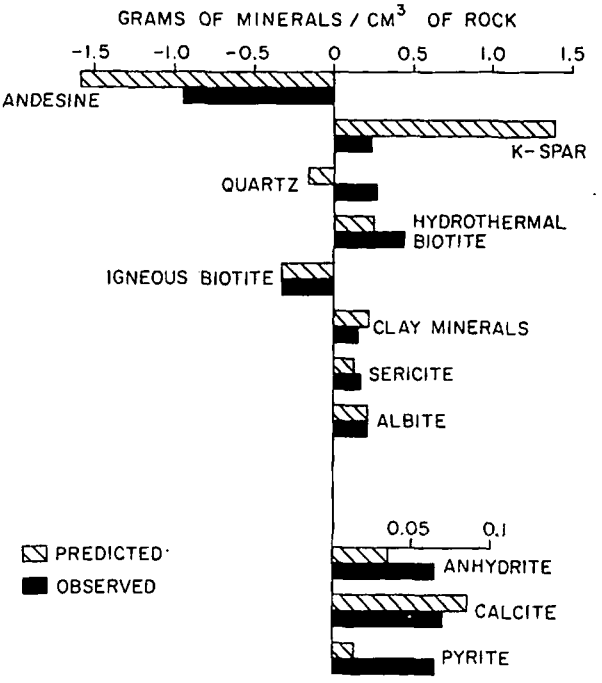

FIG. 33. Comparison between observed mineral gains and losses in the Mayflower stock and those predicted on the basis of irreversible mass transfer calculations between 300°C and 150°C and fluid-flow computations.

TABLE 9. Predicted Gains and Losses of Minerals on the Basis of Irreversible Mass Transfer Calculations between 300° and 150°C and Fluid-Flow Computations

	Length = 700 m (vertical section)					
Temperature	300°C	250°C	200°C	150°C	Total predicted	Total observed blocks 1 & 4
Mineral	Grams of minerals/cm³ of rock					
Andesine	-6.1×10^{-2}	-9.4×10^{-1}	-4.2×10^{-1}	-1.6×10^{-1}	-16×10^{-1}	-9×10^{-1}
K-feldspar	8.5×10^{-2}	1.35	-3.2×10^{-2}	-1.2×10^{-2}	14×10^{-1}	2×10^{-1}
Quartz	-2.0×10^{-2}	-3.4×10^{-1}	1.7×10^{-2}	1.8×10^{-1}	-1.6×10^{-2}	3×10^{-1}
Anhydrite	0.8×10^{-2}	3.5×10^{-2}	trace	—	4×10^{-2}	7×10^{-2}
Calcite	—	0.1×10^{-4}	6.3×10	2.3×10^{-2}	9×10^{-2}	7×10^{-2}
MF-biotite	0.9×10^{-2}	2.3×10^{-1}	—	2.0×10^{-2}	3×10^{-1}	4×10^{-1}
Ig. biotite	-1.2×10^{-2}	-2.3×10^{-1}	-4.4×10^{-2}	-2.8×10^{-2}	3×10^{-1}	3×10^{-1}
Pyrite	0.4×10^{-2}	0.8×10^{-2}	1.6×10^{-3}	trace	1×10^{-2}	7×10^{-2}
Clay minerals[1]	2.5×10^{-3}	—	1.4×10^{-1}	8.7×10^{-2}	2×10^{-1}	2×10^{-1}
Magnetite	-1.0×10^{-3}	-2.9×10^{-3}	1.9×10^{-2}	3.4×10^{-3}	2×10^{-2}	-3×10^{-2}
Sericite	1.7×10^{-4}	3.5×10^{-4}	2×10^{-1}	3.1×10^{-2}	1×10^{-1}	2×10^{-1}*
Low albite	—	—	1.9×10^{-1}	2.8×10^{-2}	2×10^{-1}	2×10^{-1}†
Chlorite	—	—	—	—	—	4×10^{-2}
Chalcopyrite			trace	trace		trace

[1] Clay minerals comprise kaolinite and montmorillonites. The observed values refer only to kaolinite.
* Value for sample MF-2801 on the 2,800-ft mine level at about 60 m south of the Mayflower vein.
† Average value of 360 m of sample along the Mayflower vein on the 2,600-ft level.

reaction path. Therefore, the effluent fluids from the stock still contained sufficient copper to produce a significant quantity of copper sulfide in the overlying host rocks.

This heuristic model of the Mayflower hydrothermal system summarizes the nature of processes which prevailed during the cooling of the stock and accounts for many of the observed geologic features. More importantly, we wish to communicate the utility of combining field observation and computer models of process to extend understanding of the processes attending formation of mineral deposits.

Acknowledgments

This research was supported by NSF Grant GA41136 and funds from the Research Corporation to Denis Norton. Financial assistance in the early stages was provided by the Research Fund of the Geology and Geophysics Department of the University of Utah, which also financed the analytical work with X-ray equipment and electron microprobe. We are grateful for valuable suggestions given by R. E. Beane, Jerry Knight, and John Delaney. A special thanks goes to Lynn McLean who greatly improved this manuscript. The data for this study were collected with the cooperation and assistance of numerous hard-rock miners, the Hecla Mining Company, and John Simos; the data were analyzed with the cooperation and assistance of the University of Arizona Computer Center staff; we thank them for their help and patience.

Department of Geosciences
University of Arizona
Tucson, Arizona 85721

Present Address:
R. N. V.
Núcleo de Ciências Geofísicas E. Geologiças
Universidade Do Pará
Belém Pará, Brazil

April 28, 1976; March 8, 1977

REFERENCES

Baker, A. A., Calkins, F. C., Crittenden, M. D., Jr., and Bromfield, C. S., 1966, Brighton Quadrangle, Utah: U. S. Geol. Survey, Geol. Quad. Map.

Barnes, M. P., and Simos, J. G., 1968, Ore deposits of the Park City district, with a contribution on the Mayflower lode, *in* Ridge, J. F., ed., Ore deposits of the United States, 1933–1967, (Graton-Sales vol.): New York, Am. Inst. Mining Metall. Petroleum Engineers, p. 1002–1126.

Beane, R. E., 1972, A thermodynamic analysis of the effect of solid solution of the hydrothermal stability of biotite: Unpub. Ph.D. thesis, Northwestern Univ., 195 p.

—— 1974, Biotite stability in the porphyry copper environment: Econ. Geol., v. 69, p. 241–256.

Boutwell, J. M., 1912, Geology and ore deposits of the Park City district, Utah, with contributions by L. H. Woolsey: U. S. Geol. Survey Prof. Paper 77, 231 p.

Brace, W. F., Walsh, J. B., and Frangos, W. T., 1968, Permeability of granite under high pressure: Jour. Geophys. Research, v. 73, p. 2225–2236.

Bromfield, C. S., Baker, A. A., and Crittenden, M.D., Jr., 1970, Heber Quadrangle, Wasatch and Summit Counties, Utah: U. S. Geol. Survey, Geol. Quad. Map.

Burnham, C. W., and Davis, N. F., 1971, The role of H_2O in silicate melts I. P-V-T relations in the system $NaAlSi_3O_8$-H_2O to 10 kilobars and 1,000°C: Am. Jour. Sci., v. 270, p. 54–79.

Burnham, C. W., Holloway, J. R., and Davis, N. F., 1969, Thermodynamic properties of water to 1,000°C and 10,000 bars: Geol. Soc. America Spec. Paper 132, 96 p.

Cadek, J., Hazdrova, M., Kacura, G., Krasny, J., and Malkovsky, M., 1968, Hydrogeology of the thermal waters at Teplice and Usti nad Labem: Sbornik Geologickych Ved Hydrology Inzenyraska Geologie, Rada Hig. Sv.6 (summary in English).

Calkins, F. C., and Butler, B. S., 1943, Geology and ore deposits of the Cottonwood-American Fork area, Utah, with contributions by V. C. Heikes: U. S. Geol. Survey Prof. Paper 201, 152 p.

Crittenden, M. D., Jr., 1965, Dromedary Peak Quadrangle, Utah: U. S. Geol. Survey, Geol. Quad. Map.

Crittenden, M. D., Jr., Stackless, J. S., Kistler, R. W., and Stern, T. W., 1973, Radiometric dating of intrusive rocks in the Cottonwood area, Utah: U. S. Geol. Survey Jour. Research, v. 1, p. 173–178.

Goranson, R. W., 1938, Silicate-water systems: Phase equilibria in the $NaAlSi_3O_8$-H_2O and $KAlSi_3O_8$-H_2O systems at high temperatures and pressures: Am. Jour. Sci., 5th ser., v. 35A, p. 71–91.

Heard, H. C., 1967, The influence of environment on the brittle failure of rocks, *in* Failure and breakage of rocks, Eighth symposium on rock mechanics: New York, Am. Inst. Mining Metall. Petroleum Engineers, p. 82–93.

Helgeson, H. C., 1969, Thermodynamics of hydrothermal systems at elevated temperatures and pressures: Am. Jour. Sci., v. 267, p. 729–804.

—— 1970, A chemical and thermodynamic model of ore deposition in hydrothermal systems: Mineralog. Soc. America Spec. Paper 3, p. 155–186.

Helgeson, H. C., Brown, T. H., Nigrini, A., and Jones, T. A. 1970, Calculation of mass transfer in geochemical processes involving aqueous solutions: Geochim. et Cosmochim. Acta, v. 34, p. 569–592.

Jacobs, D. C., and Parry, W. T., 1976, A comparison of the geochemistry of biotite from some Basin and Range stocks: Econ. Geol., v. 71, p. 1029–1035.

Nash, T. J., 1973, Geochemical studies in the Park City district; I, Ore fluids in the Mayflower mine: Econ. Geol., v. 68, p. 34–51.

Norton, D. L., 1972, Concepts relating anhydrite deposition to solution flow in hydrothermal systems: Internat. Geol. Cong., 24th Montreal, sect. 10, p. 237–244.

Norton, D. L., and Knapp, R., 1977, Transport phenomena in hydrothermal systems: Nature of porosity: Am. Jour. Sci., v. 277, p. 913–936.

Norton, D. L., and Knight, J., 1977, Transport phenomena in hydrothermal systems: Cooling plutons: Am. Jour Sci., v. 277, p. 937–981.

Quinlan, J. J., and Simos, J. G., 1968, The Mayflower mine, in Park City district, Utah, *in* Erickson, A. J., ed., Guidebook no. 22: Geol. Soc. Utah, p. 40–55.

Robie, R. A., and Waldbaum, D. R., 1968, Thermodynamic properties of minerals and related substances at 298.15° K (25°C) and one atmosphere (10^{13} bars) pressure and at higher temperatures: U. S. Geol. Survey Bull. 1259, 256 p.

Snow, D. T., 1968, Rock fracture spacings, openings, and porosities: Jour. Soil Mech. Foundations Div., Am. Soc. Civil Engineers, v. 94, p. 73–91.

—— 1970, The frequency and apertures of fractures in rocks: Internat. Jour. Rock Mech. Mining Sci., v. 7, p. 23–40.

Villas, R. N., 1975, Fracture analysis, hydrodynamic properties, and mineral abundance in altered igneous rocks at the Mayflower mine, Park City District, Utah: Unpub. Ph.D. thesis, Univ. Utah, 254 p.

Williams, N. C., 1952, Wall-rock alteration, Mayflower mine, Park City, Utah: Unpub. Ph.D. thesis, Columbia Univ., 58 p.

Wilson, J. C., 1961, Geology of the Alta stock, Utah: Unpub. Ph.D. thesis, California Inst. Technology, 236 p.